An Experimental and Numerical Investigation on the Hardness and Deformation Behavior of Particle Reinforced AMMC

A Dissertation submitted

in the partial fulfillment of requirements

for the degree of

MASTER OF ENGINEERING

in

CAD/CAMENGINEERING

by

SHIVAM SAINI

801584017

Under the guidance of

Dr. Hiralal Bhowmick

Assistant Professor, MED

MECHANICAL ENGINEERING DEPARTMENT

THAPAR UNIVERSITY, PATIALA

July, 2017

CERTIFICATE

This is to certify that the thesis entitled, **"AN EXPERIMENTALAND NUMERICAL INVESTIGATION ON THE HARDNESS AND DEFORMATION BEHAVIOR OF PARTICLE REINFORCED AMMC"** is an authentic recordofmy workcarriedoutas requirement for the award of **Master of Engineering** in**CAD/CAM Engineering**submitted at **Thapar University, Patiala** under the guidance of **Dr. Hiralal Bhowmick**, Assistant Professor, Mechanical Engineering Department, Thapar University, Patiala July, 2016 to July, 2017.The matter embodied in this present work has not been submitted in part or full to any other university or institute for the award of any degree.

Date: 09-08-2017

Shivam Saini

This is to certify that above declaration made by the students is correct to the best of our knowledge and belief.

Dr. Hiralal Bhowmick
Assistant Professor
Mechanical Engineering Department
Thapar University, Patiala -147004

Dedicated

To

My Beloved Parents

Acknowledgement

I express my sincere gratitude to my guide **Dr. Hiralal Bhowmick, Assistant Professor, Mechanical Engineering Department, Thapar University, Patiala** for his invaluable guidance, proper advices, painstaking and constant encouragement during the course of my work on this seminar.

I am greatly thankful **to Dr. S. K. MOHAPATRA, Sr. Professor and Head, Department of Mechanical Engineering** for his encouragement and inspiration for execution of the work.

I am also very thankful to the specially Mr. Nariendra Singh, Lab Assistant, entire faculty and staff members of Mechanical Engineering Department for their direct- indirect help and cooperation.

A special thanks to Harpreet Singh, Ph.D. scholar and my friend Parampreet Singh, Gaurav Sharma and Ripan sarkar for their help and support during thesis work.

In the end, I wish to express my profound sense of gratefulness to my family, for supporting and encouraging me at every step of work. It is their blessings, which has given me the mettle, confidence and enthusiasm for hard work.

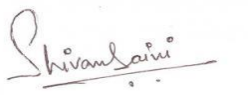

Shivam Saini

Abstract

Today's requirement and demands cannot be accomplished by alloys and metals alone e.g. trusses, branches used for making satellites need to be dimensionally stable between wide ranges of temperatures. These days Metal Matrix Composites (MMC) replaced conventional materials (metals) in many applications due to their superior properties such as light weight, strength to weight ratio, hardness and stiffness, wear, corrosion resistance and withstand with high temperature over conventional materials. Nowadays stress to use lightweight materials has increased because of environmental issues. Some of the examples of components that have been manufactured using metal matrix composites include pistons for diesel engines and connecting rods. Aluminum Material Matrix Composites (AMMC) had superiority over other conventional materials in the field of aerospace, automotive and marine applications owing to their excellent improved properties. These materials are of much interest to the researchers from few decades. These composites initially replaced Cast Iron and Bronze in many applications. With rapid increase in usage of composite in practical application, it is of great interest to do the failure and deformation analysis of these developed materials. However, due to the complexities involved and computational resources required in the analysis, the research in this area is still in the emerging stage.

In this present work an attempt has been made to investigate the hardness and deformation behavior of particle reinforced AMMC using numerical and experimental approach. AMMC for experimental investigation are fabricated using stir casting procedure. SEM, EDS and XRD validate the uniform distribution of Al-SiC(10% wt.) composite obtained by stir casting. Mechanical properties such as the microhardness, nanohardness of the composite are selected for the investigation. Microhardness and nanoindentation test has been successfully done on the Al-SiC composite. CAD modeling and simulation have been developed for predicting the hardness of the composite. Axisymmetric model is used for the simulation of nanoindentation whose results has been validates with the experimental data. Based on experiment and simulation results, hardness value has been obtained from the depth of penetration. In addition, the deformation behavior of composite under tensile loading is also investigated with experimentation and simulation. Simulation of particle reinforced MMC has been done through image based modeling. Validation of simulation results obtained through SEM images of deformed surface.

***Key words**:* Metal Matrix Composite (MMC), Nanoindentation, FE Simulation, Microstructure Image Processing, Deformation.

CONTENTS

List of Figures

List of Tables

Nomenclature

d= distance between lattice planes

Θ= angle between diffraction waves

n= numeric constant known as order of diffracted beam

λ= wavelength of beam

H_v=Vicker Hardness

F= load in kgf

d_{mean}= Arithmetic mean of the two diagonal, d_1 and d_2 in mm

h_c= contact penetration depth, nm

h_m= maximum contact penetration depth, nm

F_m= Maximum load applied during nanoindentation, μN

E_i= Indenter Young's Modulus of Elasticity, GPa

v_i= Indenter's Poisson's Ratio

Acronyms

MMC	=	Metal Matrix Composite
AMMC	=	Aluminum Metal Matrix Composite
FEM	=	Finite Element Method
DRAMMC	=	Discontinuous Reinforced Aluminum MMC
PAMMC	=	Particle Reinforced Aluminum MMC
SiC	=	Silicon Carbide
TiC	=	Titanium Carbide
B_4C	=	Boron Carbide
SEM	=	Scanning Electron Microscope
XRD	=	X- Ray Diffraction
EDS	=	Energy Dispersive Spectroscopy
DEM	=	Discrete Element Model
RVE	=	Representative Volume Element
CSM	=	Continuous Stiffness Measurement

Chapter 1

Introduction

1.1 Introduction to Composites

Composite is a material which needs minimum two different constituents. The constituents are united at a macroscopic level and are not soluble in each other. The primary constituent is called the matrix that provides load transfer and structural reliability, while the other constituent is reinforcement to enhance mechanical properties. The constituent of the composites materials can either be organic, polymer, inorganic or metallic and ceramic. The reinforcing phase may be of fibers, particulate or whiskers, flakes. The most common forms of reinforcement materials are fibers or particulates. Generally, the matrix phase materials are continuous in nature. Wood and bone are naturally found composites.

Composite materials have superior specific properties compared to metals. It is well known fact and most of researches conclude it in their researches [1]. Now-a-days composites are replacing conventional materials for many engineering applications due to their superior properties such as high strength to weight, high stiffness as well as better damage resistance over a wide range of operating conditions, excellent fatigue resistance, high heat resistant, high wear resistant, high corrosion resistant, etc. With the help of suitable arrangement while adding reinforcement and matrix, we can achieve desired properties of composites for a particular application.

The strong growths in the field of composites have been widely affected by multifunctional design requirements. The conventional attitudes for the development of a load-bearing structure need to address the every function requirements separately, resulting in the growth of the multifunctional materials, which are undoubtedly the composite materials [2].

Advanced composites are used in the aerospace industry having high performance reinforcement of thin diameter in a matrix material such as epoxy and aluminum. Trusses and benches used in satellite needs dimensionally stable in space due to variation in temperature. Metals cannot meet the demands of today’s advance technologies, only combining different materials but perform their task.

The functions of matrix are to bind the reinforcements together and to distribute the load to reinforcement. It also influences the various mechanical and thermal properties such

as compressive and shear strength, modulus, thermal expansion coefficient, thermal resistance, fatigue strength, etc. Material of reinforcement, length, orientation, shape, chemical, mechanical properties and reaction bonding with matrix influence performance of composite.

1.2 Classification

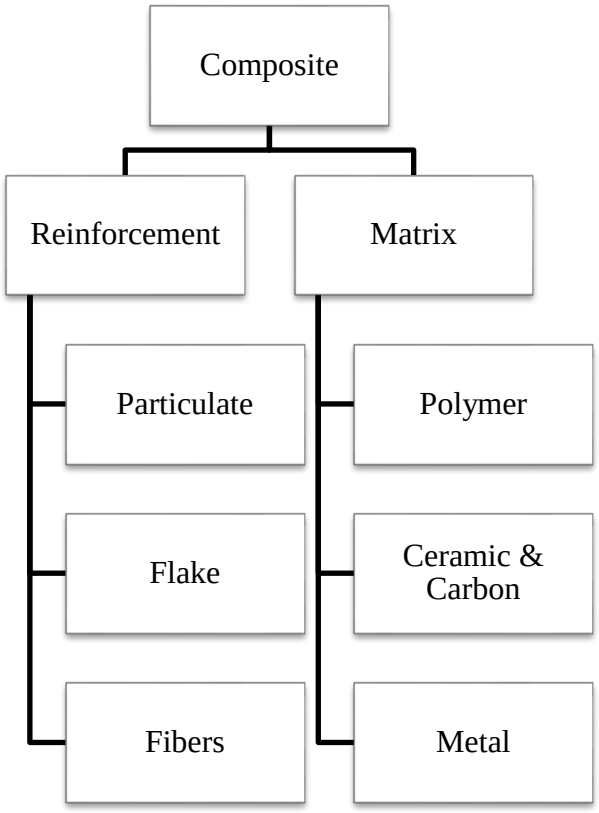

Figure 1.1: Basic classification of composites [1]

The composite is broadly classified on the basis of reinforcement and matrix material used. There are various types of reinforcements and matrix material present due to very rapid growth and interest of industry in composites. Last decades huge amount of researches havebeen done on different type of fabrication in composites field according to the desired needs.

One or more material particles can be suspended in binding matrix of particulate composites. A particulate by definition is not long or have short in dimensions. On the basis of orientation particulate composite can categorize as random and preferred orientation. Particulate composite do not have high fracture resistance unlike fibrous composite. Fibrous

composites consists reinforcing fibers deferred in binding matrix. Nothing like particles, fibers have high length to diameter ratio. Single layer fibers are oriented in the particular direction. Further advancement in layer and form stack of such layers eventually form a composite material. Multilayer phenomena provide different reinforcements at each layer and in hybrid laminates multiple material sheets/ laminates make a composite.

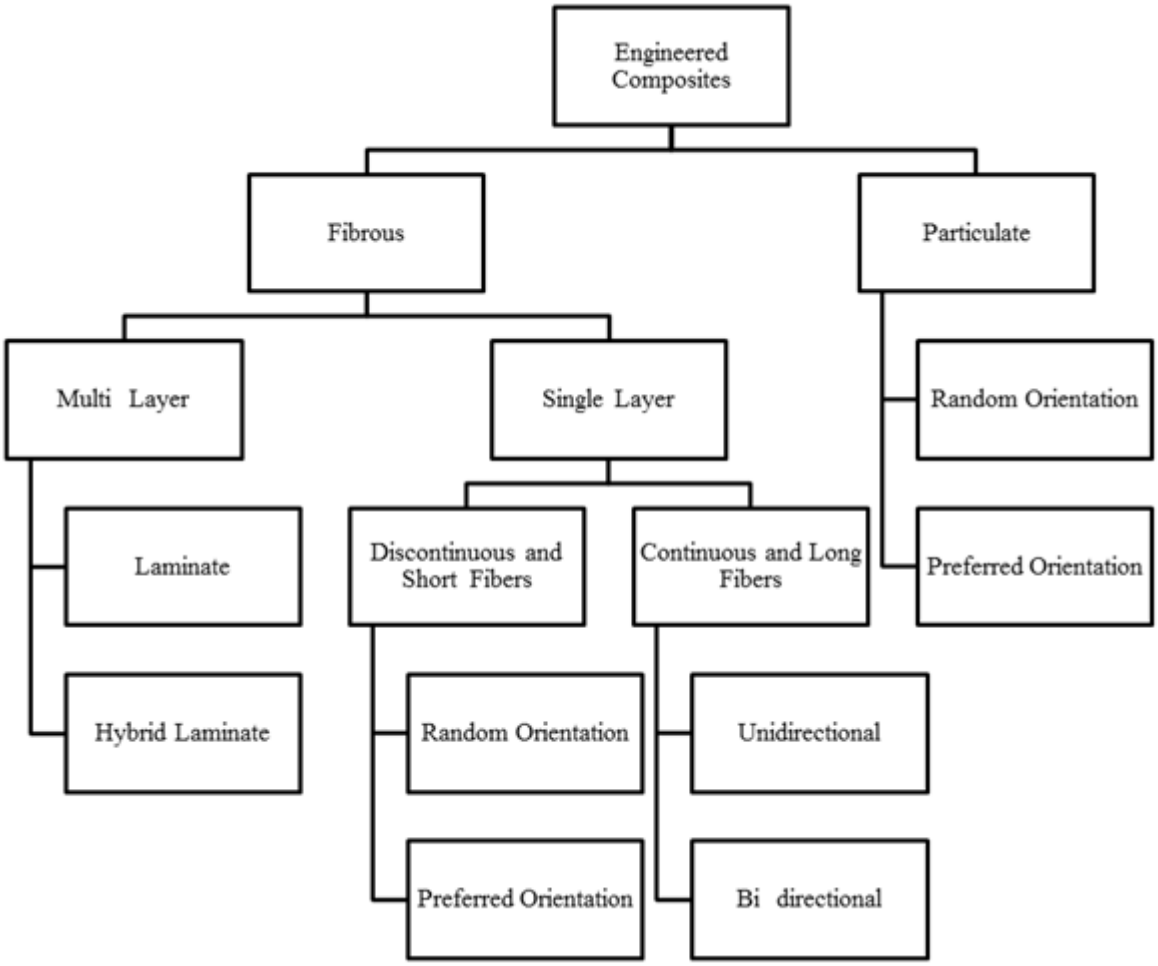

Figure 1.2: Detailed classification of composites [1]

A composite reinforced with fiber reinforcement is known as fibrous composite and with particles as reinforcement is called particulate composite. Fiber reinforcements of a thin diameter are preferred because it decreases flaw and increases strength. It also provides large surface area for reinforce-matrix interface.

Some considerations have to be kept in mind while selecting material matrix such as modulus, strength, conductivities etc., curing temperature of material, viscosity, reactivity of reinforcements with material into composite system and environment, fabrication process compatibility and cost. Structural applications demands a range of superior structural

properties like strength, stiffness, fracture toughness, damping, etc. On the other hand, non-structural application demands electrical and/or thermal conductivity, sensing and actuation, energy harvesting/storage, self-healing capability, recyclability and biodegradability [2].

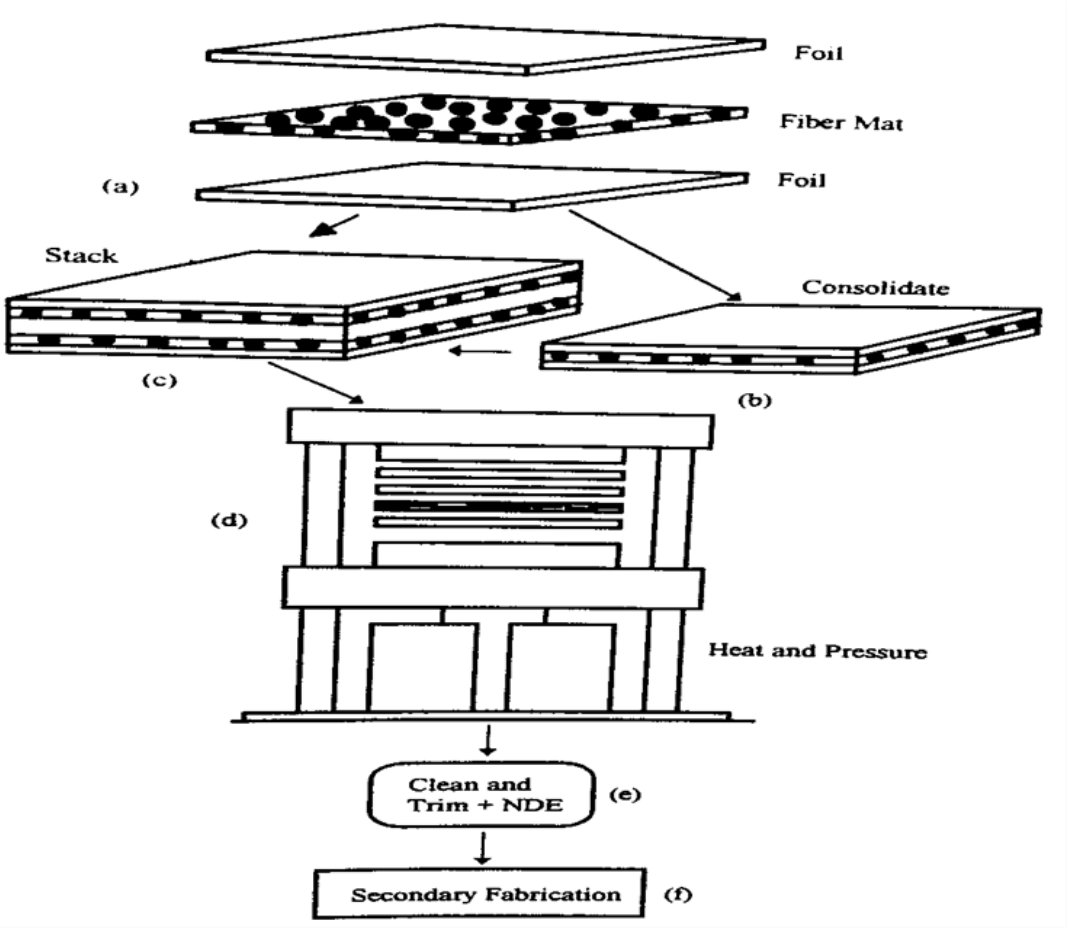

Figure1.3: Layer by layer fabrication processes [1]

1.3 Metal Matrix Composites (MMC)

Matrix material in MMC commonly used are Al, Mg, Cu, Ti and their alloys. Reinforcement materials in MMC are silicon carbide, boron carbide, alumina and graphite in the form of particles or fibers. MMCs are mainly used to provide advantage against monolithic metals such as steel and aluminum. MMCs include higher elastic properties, service temperature, electric and thermal conductivities, insensitivity to moisture, better wear fatigue and flaw resistance. MMCs used in space shuttle, military for missile guidance system, automotive engines to reduce the weight. Metal matrix properties can be altered with the addition of different type of hard and soft reinforcement materials in the form of particles or

whiskers.Particulate reinforced composites having less production cost compared with fiber reinforced composites. The particulate material physical properties are isotropic in nature.

1.3.1 Aluminum as Matrix Material and Various Aspects of AMMC

Aluminum has advantage over other materials in the sense of light weight. With the addition of the different reinforcements, desired properties of different nature or application can be achieved. Composites of aluminum have reinforcement in form of discontinuous/continuous fibers, whiskers or particulates with different volume fraction. Aluminum Metal Matrix Composites (AMMC) also gives flexibility with processing routes, matrix combinations on the demand of industrial application [3]. Advantage of AMMC compared to unreinforced material include reduced density, improved strength and stiffness, high temperature properties, abrasion and wear resistance, damping capabilities, electrical performance, controlled thermal expansion coefficient and control of mass especially in reciprocating parts.

For automobile industry low fuel consumption, less noise and lower airbone emissions are some of the benefits of AMMC. With regular increment in environmental guidelines it has been a great challenge on the industries to emphasis on improved fuel economy. Besides, use of AMMC in transport sector is inevitable. According to United Kingdom advisory council on S&T, AMMC will be a replacement of existing material. Particulate AMMC are more or less isotropic in nature and homogenously distributed, due to which easily subjected to secondary forming process like extrusion, rolling and forging [4].

1.3.2 Alloys and Reinforcementused in AMMC

Aluminum alloys are being extensively used in various fields of life, especially in aerospace and automobile industries, because of good thermal stability and excellent specific strength. Now days it is used in space industries for insulation and light weight, precision components of missile guidance systems, engine parts in automotive industries, turbines blades, airplanes etc. In AMMC, matrix material is aluminum or its alloys and reinforcement materials are carbides, oxides and graphite etc. in the form of fibers, whiskers and particles as shown in Figure 1.4. These AMMC with multiple reinforcements (hybrid MMCs) enlarged the applications in the field of road transportation, aerospace, marine, automobile and mineral processing industries. It is due to reason that mechanical and tribological properties of composites. Hence it acts as better options in lieu of single reinforced composites.

Commercial aluminum alloys are selected for MMCs on the basis of good mechanical properties, easily available and suitability for heat treatment. The common series ofaluminum

alloys broadly used for MMC applications are 2000 (Al-Cu), 4000 (Al-Si), Al (6061), 5000 (Al-Mg) 6000 (Al-Si-Mg) and 7000 (Al-Zn- Mg).

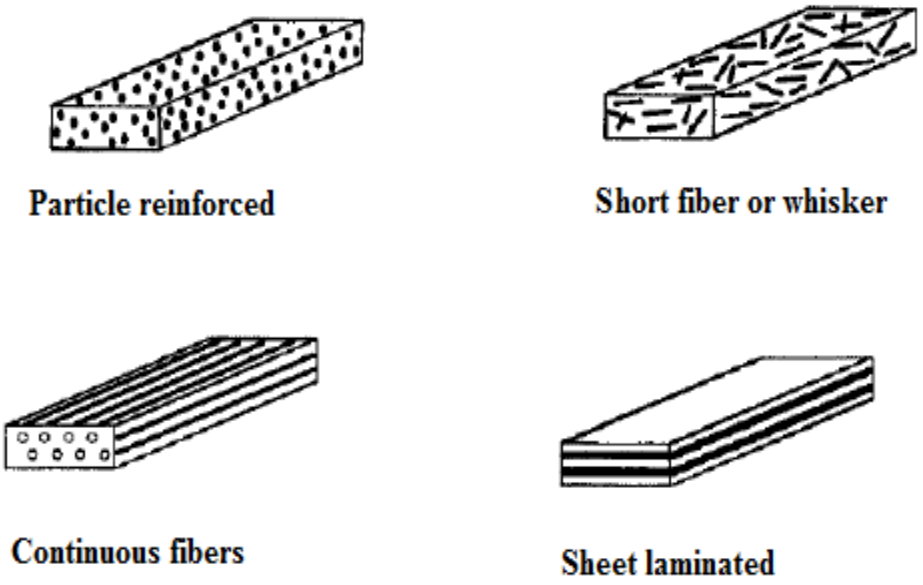

Figure 1.4: Different types of reinforcements

Necessities for reinforcement are having low densities which make it soluble, compatibility with matrix alloy leads to better strength, chemical compatibility decreases the chances of chemical reaction, thermal stability protects it from temperature variation, high compression and tensile strength makes it reliable, economic efficiency saves money and cost. Discontinuous Reinforced Aluminum MMCs (DRAMMCs) or Particle Reinforced Aluminum MMCs (PAMMC) are easy to manufacture and widely used in the industry. Reinforcements made of ceramics like silicon carbide (SiC), titanium carbide (TiC) and boron carbide (B_4C) particulate are brittle in nature due to high hardness. So generally they are used in particulates form. PAMMC generally reinforced with ceramic which are carbides, borides or oxides maintaining aspect ratio less than 5. Powder metallurgy (solid state), Stir casting, in-situ(liquid state) are most commonly used methods for manufacturing PAMMC. PAMMC obtained through these methods are isotropic and can be easily used in secondary operations [5]. Short fiber whisker reinforced and continuous fiber reinforced composites are used nowadays but in very limited way. They required specialized manufacturing techniques.

1.3.3 Mechanical Characterizations of AMMC

There are various properties which can discuss by researches in their studies but the major ones are hardness and tensile strength. Also composite especially metal composites are tailored to attain certain properties as per the requirement where it uses.

- Hardness: Resistance of material against surface indentation termed as hardness. It emulates interface bonding strength of composite's constituents. The presences of hard particles (SiC) which are well connected to the matrix (aluminum) reduce the dislocation and tighten the structure causes improvement in hardness. Testing of micro hardness is done through Vicker hardness test and Brinell hardness test in most of the researches.
- Tensile Strength: With the increase of weight percentage of reinforcement porosity increases. But an increase in porosity is manual defect and controlled by improvements in method. Interfacial bond contributes to enhance the tensile strength of AMMC's [5]. Segregation of SiC particles causes low tensile strength sometimes. Short fibers improve tensile strength and modulus of the MMC's. Testing of various weight percentage of AMMC is done through normal universal testing machine.
- Impact Strength: With the increase in the weight percentage of reinforcement impact strength of the composite increases. But, there is a limitation of concentration up to which reinforcement should be added in the matrix. Testing of impact is done through charpy test in which hammer with weight is strike through the composite.

1.4 Microstructural Characterizations of AMMC

Microstructural studies of various composites are done through SEM, EDS techniques. Scanning Electron Microscopy (SEM) is used to determine the surface morphology, layers and inclusions. Energy Dispersive X-ray Spectroscopy (EDS) identifies the different elements types formed and their percentage in prepared sample, the microstructure analysis can identify inclusions type and corrodes on the fracture face. Relevant techniques such as SEM, XRD, EDS and optical micrographs used to study the microstructures of composites.

1.5 Methods of Manufacturing AMMC

Conventional monolithic materials had some certain limitations in attaining better combination of various mechanical and physic-thermal properties. For improving these deficiencies, combination of two different types of material is used. For fulfilling the rapid increase in demand of modern day technology, usages of composites are the one of most

trending solution of recent interest. Some commonly used method used for fabrication of MMCs is described below.

Stir casting method is also known as liquid state fabrication of MMCs. It encompasses dispersed phase embedded into a molten matrix metal, trailed by controlled solidification. For providing enhanced level of mechanical properties composites must have good interfacial bonding (wetting) between the reinforcements and the liquid matrix. Stir casting economically attains these qualities. With the help of coating, the dispersed phase particles wetting improvement can be achieved by reducing the chemical interaction between the dispersed phase and the matrix. This also helps in the reduction of interfacial energy. The stir casting is the one of the most cost effective with uniform distribution, method of liquid state fabrication of MMCs.

Amongst the various manufacturing processes available stir casting is a particularly promising route due to its flexibility, simplicity and applicability to large volume production. It minimizes the cost of the production and allows very large sized components to be produced. In preparing MMC through stir casting uniform distribution, wettability, porosity and chemical reactions between reinforcement -matrix alloy are some factors which need attention [6]. Figure 1.5 shows the schematic diagram of the stir casting setup.

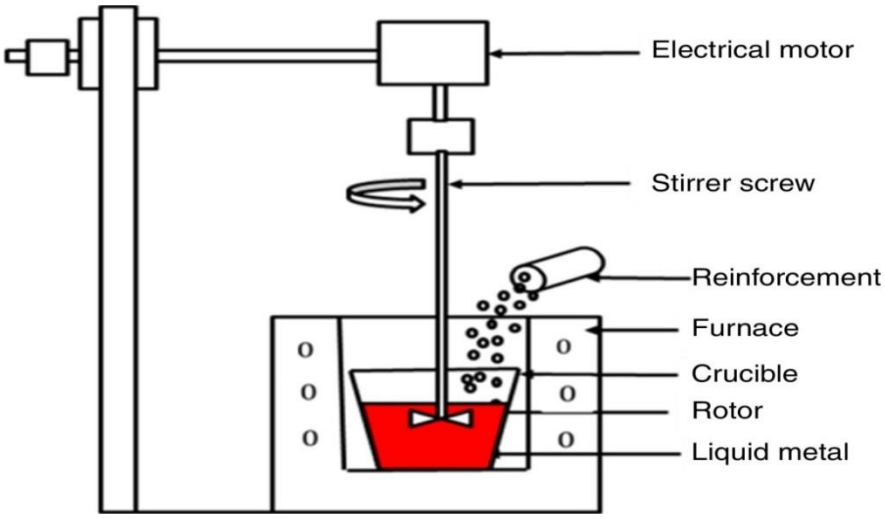

Figure 1.5: Schematic diagram of stir casting set-up

The distribution of reinforcements influences through distribution in liquid at mixing, after mixing and redistribution as result of solidification. But vortex method established as best approaches for good distribution in composite. After study different designs of stirrers, turbine stirrer is mostly used because of transferring particle into liquid metal and

maintaining particle in state of suspension [7]. Cast composite's properties are influenced by the processing parameters such as air and impurities entrapped into liquid, holding temperature, stirring speed, size of impeller and the position of impeller in melt [8].

Powder metallurgy is the process of mixing fine powdered materials. These fine powdered materials are heated at certain temperature and pressed into certain shape and size. Then, in a controlled atmosphere heating of the compressed material or green sample is to be done to bond the material (sintering). The powder metallurgy processes generally have four simple levels i.e. powder manufacture, powder blending, compacting and sintering. Compacting is executed at normal temperature and sintering is usually conducted at the elevated temperature process and atmospheric pressure [9]. Better properties and improved precision can be obtained from the optional secondary process. This process also reduces cost of material removal process. Pre-determined shape and size of die produced final products without any material wastage.

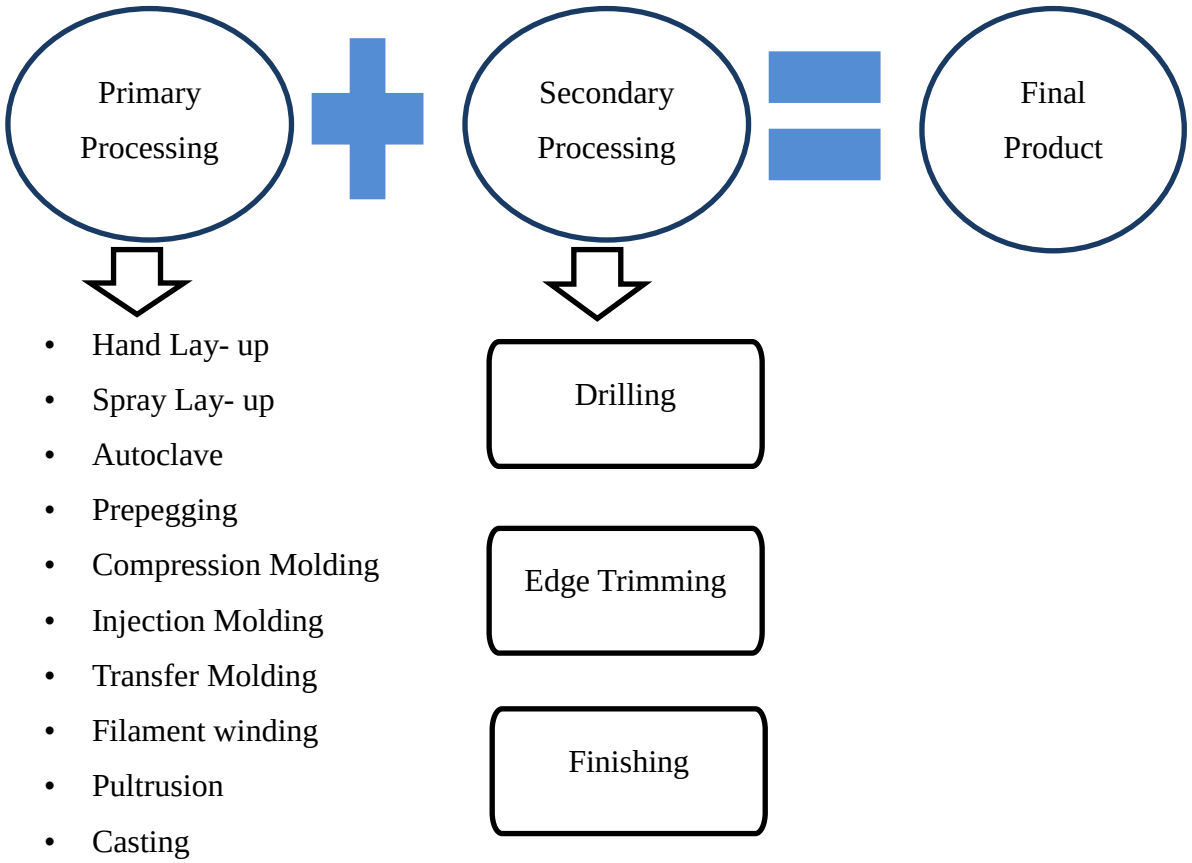

Figure 1.6: Manufacturing process for composites

Some other processes are as shown in Figure 1.6. For each and every process some advantages and disadvantages are always present. But the limitation of these processes lead to other methods. Characteristics and limitation of each processes defines its use. So, according to the desired need processes can be opted by the manufacture.

1.6 Application of Aluminum Metal Matrix Composite

Al 6061 is widely used in industry due to their good mechanical properties and wettability. Nowadays its uses in aircraft's wings, fuselages, yacht and utility boats, tactical flashlights, scuba tanks, coke cans etc. [1, 10]. But automotive industry uses aluminum on full scale and unearthed many properties of aluminum by making composites from it. Due to low weight high strength ratio aluminum alloys used in automobile industry [2-5]. AMMCs are now regularly used in the parts of passenger cars, in interior headliners, underbody systems, bumper beams and instrumental panels [11, 12]. Moreover, high performance composite materials are in growing demand in racecar and high-performance vehicle components as well as the requirement of lightweight vehicles are the primary driving factors for the increase in composites penetration in the automotive industry [11]. By using aluminum in the body and structure of Ford F-150 pickup, Ford claims a weight reduction that exceeds 318 kg. In 2014, GM signed major contracts to convert its line of pickups from steel to aluminum in 2018[12]. Figure 1.7 shows the areas where composite used and estimated increase in future.

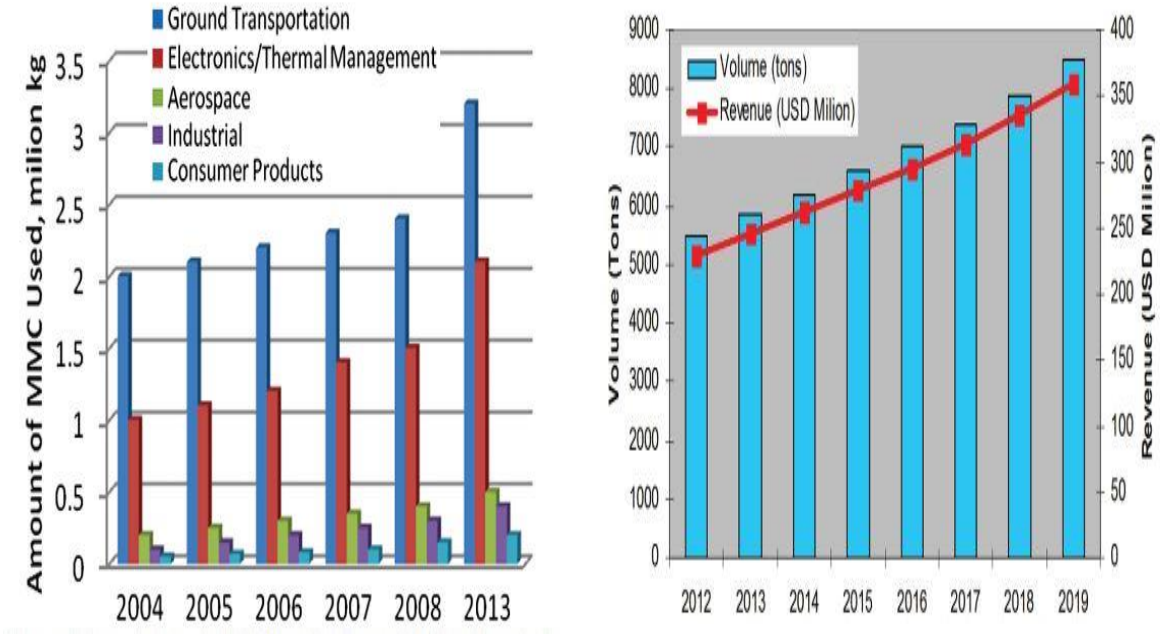

Figure 1.7: Amount of composite used in past and future requirement [12]

Automotive engine components like cylinder blocks, pistons, disc, cardan(drive) shaft, connecting rod, brake drums, and piston insert ring, calipers, gears, valves, turbine, housing of pumps etc. all have operated in condition where adhesive and abrasive wear are main mechanism of dry sliding wear. These also required heat- water resistance, high stiffness to fatigue and must be lightweight for lower the fuel consumption with better efficiency.

Pistons having hard thermal and mechanical environment conditions where cyclic load with high (100Hz) frequency causes fatigue. They also provide an intimate contact with cylinder which requires high resistance to wear and thermal expansion of coefficients. AMMCs have these properties with high thermal conductivity to resist effects of these conditions [13]. Also, summary cost of traditional piston is higher than composites piston. Toyota uses pistons for diesels engine. MMC based cylinders firstly used in Honda prelude (Al+ Alumina 12%+9%C). They give better results with less thickness of barrel cylinder and increasing volume of expansion. In case of connecting rod with aluminum MMC 57% of weight reduction is observed. Vibration, energy loss and load on crankshaft also decrease. Nissan was the first company to use it Al-SiC composite in case of connecting rod. In case of brakes, Al-SiC and Alumina uses in Volkswagen, Toyota, and General Motors cars. In Germany intercity expresses trains uses AMMC brakes. Cardan shaft/ drive shaft requires transmitting torque, it converts reciprocating motion into rotation. So it requires high stiffness but it became unstable at critical speed. Critical speed is functions of speed, length, outer and inner diameter and stiffness. With the Al6061-Alumina or SiC through stir casting, stiffness of the shaft increases [13].Figure 1.8 shows the automobile parts made from Al-MMC.

Figure 1.8: Pistons, Push rods made from Aluminum metal matrix composite [12]

With the increase in technology hybrid cars, electric cars, satellite panels, rotating blade sleeves in helicopter, flight control hydraulic manifolds, trains and cars braking systems golf club shaft, skating shoes, baseball shafts, horse shoes and bicycle frame, microwave plate and its housing all requires less weight for better efficiency.

1.7 Deformation Mechanics and Modeling Mechanical Behavior of Composites

It is established fact that composite materials have certain advantages due to dispersion of micro reinforcement into the base material which offered properties and functionalities more superior than the traditional material. There are two approaches used in modeling behavior i.e. discrete or distinct methods for molecular dynamics simulation and continuum methods using finite element methods. A discrete method includes three components in molecular dynamic simulation. First is set of initial conditions in which primary locations and rates of particle in the system were defined. Second was a force among all the particles to represent interaction potentials. Another one which is not so famous due to large routine of calculation, is solving the numerically with the Newtonian equations. MLPG- Eshelby Method is an enhanced discrete element model (DEM) for heterogeneous model. DEM had faster convergence rate as compare to FEM while investigating deformation and fracture mechanisms but it neglects some of the important factors [14].

In early 1970's use of FEM was introduced to predict mechanical properties of composite material. Various models depending on the ease of obtaining result and conditions are developed till now. The Representative Volume Element (RVE), Unit Cell Method and Object Oriented Modeling are the FEM approaches which are generally used in past to analyzing and characterizing the composites. The RVE is modeled as a rectangular solid whose entire volume is taken up by the matrix, and the filler material is modeled as a three-dimensional (3D) elastic beam. The 3D solid elements and beam elements are used to model the matrix and filler material, respectively. In RVE the behavior of the isolated reinforcements are simulated using the progressive fracture model whereas the filler model act as a space frame structures. The nodes of matrix and filler material are bound together.

While unit cell method is special case of RVE model in which a number of fillers are analyzed over a large area as compare to RVE. In this researches used 2D and 3D modeling with both periodic and symmetrical boundary conditions. In both the approaches certain assumptions are made i.e. shape of fillers are pre-defined such as spheres, cylinders,

ellipsoids or cubes. So, these problems are resolved in image based modeling where actual microstructure of the composite is necessary to predict the overall properties.

1.8 Image Processing

Raster image is defined through pixels. Each special place or location element has a pixel. Pixel is defined as the infinitesimally small cuboid which contains properties in the form of color or segment of whole image. Raster image normally obtained through the optical scanner, digital camera and other raster imaging devices. The specific resolution is obtained by the limiting resolution of the method and the source's data quality. Raster image having pixels at all particular locations, due to this reason it limits the particular area it can represent. By doubles the resolution, size become four times due to the pixel in X and Y dimension gets doubled. Vector data is in the form of points and lines which are interrelated to geometrically and mathematically. Coordinates of point as (x, y), whereas lines are represented through chain of points. A straight line is made from two points having coordinates (x_1, y_1) and (x_2, y_2).

In general, vector data file size is much smaller than raster image. It is due to the fact that coordinates saved in the vector data form. It is even truer in case of graphic or images where primary interests are boundaries and shapes rather than large homogenous regions. Conversion of raster to vector data called vectorisation process. From the last decades there is extensive research which focuses on the fast and accurate raster to vector conversion. A complete conversion process consist several steps like image acquisition, pre- processing, tracing, extraction, recognition, and topology. The quality and accuracy of the vectorized data's key factors are resolution and quality of raster image.

Concentrating on edge detection technique, it serves essential part of many computer vision systems. Since image processing had a high computational technique, various efforts have been made to reduce the size of calculations and data. The edge detection technique is simply the process of reducing the size of calculation drastically by reducing amount of data to be processed.Canny edge detection based on two criteria's i.e., detection and localization. It must be significant that corners or edges occurred in the image never be neglected and no specious responses from them.

The other criterion is related to the localization of edges points. It means that there will be minimum distance between points marked by the detector and the "center" of the true

edge. After detection and localization with the help of numerical optimization technique the obvious edge points selected and eliminating multiple responses [15].

By further enhancing the canny edge detection benefits of similarities in the filter's responses at adjacent scales are taken into consideration. The new scheme multiplies the responses to enhance edge structures. Localization accuracy and yield better edge detection results are improved with the help of scale multiplication [16]. Basic steps followed in the canny edge detection step are described in the Figure 1.9.

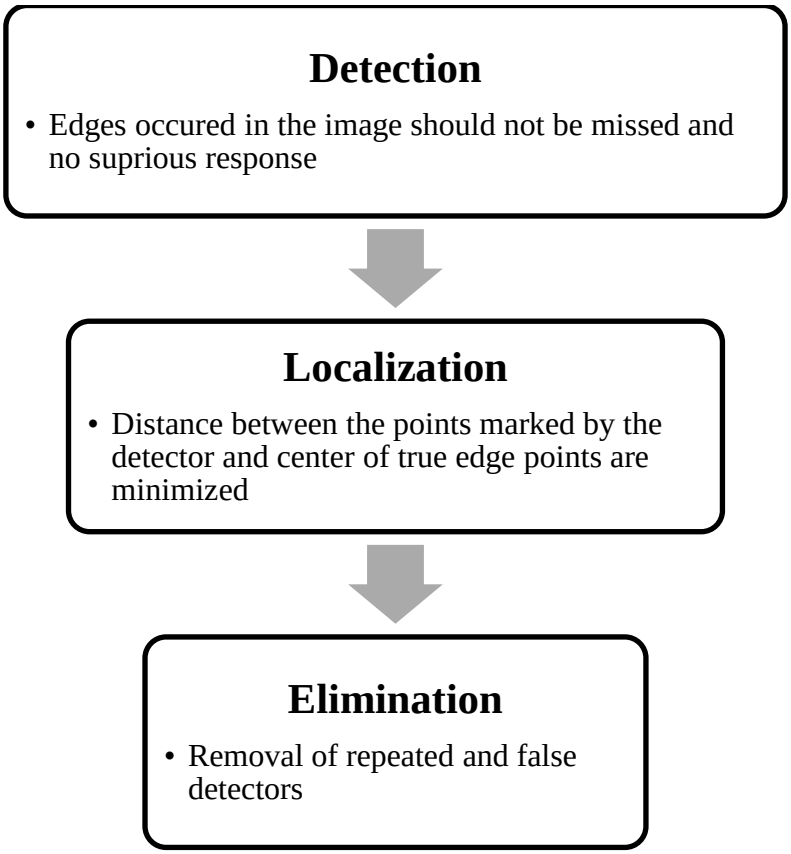

Figure 1.9: Canny edge detection step

Chapter 2

Literature Review

2.1 Introduction

The most common procedure to manufacture different kind of MMC is stir casting. Different types of reinforcement used widely in composites with different shape and sizes. In particle reinforced composite manufactured by stir casting have a property of random orientation of particles in matrix. These particle orientations in the matrix affect the properties of composite. Here brief study has been done on the different procedures related to PAMMC modeling and simulation to investigate the effect of loading on deformation and microstructure distortion.

2.2 Literature Review on the Modeling of PAMMC

There are several attempts made to develop a model for mechanical behavior of metals and particle reinforced metal composites. Some of the attempts based on microstructure based base modeling are discussed as below.

Prabhu and Karunamoorthy [17]presented microstructure based simulation used to predict the micro level stress distribution. He ensured in its study about the stress-strain behavior and failure mechanisms through 2D microstructure based FEA. He investigated the influence of clustering and particle geometry on strength. He also compared random particle with particle clustering microstructure. Fabrication of MMC samples done through stir casting method to get random distribution and clustering of particles. For finite element analysis, microstructure simplified to vector format from raster format. After that vector format converted to CAD file format and fed into analysis software. The reinforcement particles SiC modeled as linear elastic and matrix Al alloy as elastic- plastic material. Value obtained through experimentally used as input for matrix and reinforcements. Effect of particle clustering on ultimate strength is done through comparing experimental data with FEA results. 20% variation was obtained due to porosity in casting MMC and variation of microstructure in test specimen. He concludes that particle fracture or interface decohesion is larger in particle cluster than random particle clustering. He also observed random particle microstructure fails due to matrix yielding. While in particle cluster failure was due to

interface decohesion and matrix yielding. They had used the following input parameters for their analysis.

Kumar and Babu[18] approached the method of developing 2D model from a microstructure image to study the deformation and failure criteria in MMC. In his research conversion of microstructure image to vector format is done through Win-Topo software which gives files in .IGES format through canny edge detection method. In his conclusion he achieved a stress- strain graph and from the slope of graph young's modulus is obtained. The observation supports the reason of failure given by authors. **Ayari *et al.***[19]carried out aFEA study of 2D and 3D microstructure based model of a MMC reinforced with ceramic particles (Fe-TiB_2). After comparing experimental and FEM results researchers conclude that microstructure based model is more close to the experimental results.

Sozhamannan *et al.*[20]analyzed two different types of SEM images (2 images with clustering and 2 images with normal distribution) to predict the strength and failure mechanism of particle reinforced MMCs (PRMMCs). SEM images were taken to investigate the processing-structure-property relationship. They concluded that particle fracture, interfaces decohesion and volume fraction and size of particles have influential effect in failure of PRMMCs.

Sabathkumar *et al.* [21] worked on the hybrid metal matrix composites and its analysis. He used Al 7075 as matrix and SiC with TiC as reinforcement. For deformation behavior of composite microstructure based analysis was used. From his analysis of uniaxial tensile loading he derived that with the increase in the volume percentage of reinforcement, strength also increases.**Chawla and Chawla** [22] conclude that 3D microstructure based method is more precise for understanding material behavior. The distribution of plastic strain with homogenous microstructure was more uniform as compared to clustered particle composite. 2D microstructure based FEA shows the anisotropy in deformation and thermal resistance stresses.**Peng and Fuguo** [23] concluded in his research that 2D microstructure based model's stress strain behavior is quantitatively consistent with experimental result. He also concludes that the strengthening behavior of material is not affected by the strain rate and temperature.**Dobrzanski *et al.*** [24] achieved a good agreement in their result to predict hardness for casting the different Magnesium alloy. Hardness of the alloys calculated experimentally through Rockwell method and then simulates same conditions in ANSYS computer simulation software. Author's motivation behind this approach is to truncate the design process and know the effects of particular factors on the model. Finite element model helps to know the relationship among various parameters and to choose optimum solution.

Diler and Ipek [25] studied the effect of matrix, volume fraction and their interactions on the flexural strength of Al-SiC MMC. Different volume fractions and particle size are used to make interested composite through powder metallurgy. The effects of factors and their interaction on the flexural strengths are calculated by the central composite design (CCD). Bending test was performed on the different composite to know the flexural strength. Through CCD author reports that there is negative influence of particle size and volume fraction on flexural strength. Volume fraction dominates over the other two factors. Highest flexural strength obtained at low reinforcement and particle size. Flexural strength decreases at low fraction due to particle clustering.

Peng and Fuguo [26] studies the effect of particle on the distortion of particle reinforced MMC with statistical method. 15% SiC reinforced composite was prepared through powder metallurgy. With the help of MATLAB, area and perimeter of each particle was calculated through image processing technique. FEM was applied to the actual microstructure and obtained contour plots of Von Misses effective stress-stain distribution in matrix and particle. While applying boundary condition one end was fixed and other was kept at 10% compressive deformation. Correlation of particle and deformation obtained through actual microstructure. Study is done on the influence of particle under the compressive behavior of material. Author concludes that the variation of maximum stress in particles and matrix depends on the particle sizes and shape factors of reinforcements.

Paknia *et al.* [27] studied the effect of size, concentration and shape of reinforcement on the behavior of metal matrix composite using aluminum- silicon carbide composite. They used four different shapes of reinforcement i.e. circular, triangle, rectangle and square. In addition of this stress- strain distribution under tensile loading and possibilities of fracture were also investigated very extensively. They used three different concentrations of low and high i.e.10%, 15% and 20% of SiC. They achieved in their result that a particular shape of reinforcement give better tensile properties and stated that stiffness of matrix not only depends on interfacial length but also on shape, size and reinforcement of matrix material which facilitated the transfer of the loads from matrix material to particles. They investigated total thirty six cases under positive displacement and reported that 10% reinforcement is negligible.The rectangular particle's MMC shows highest stiffness as compare to the other MMCs and strain pattern was most widely and evenly distributed in the matrix around rectangular particles.

Table 2.1 summarizes the key findings of the significant works carried out by the various researchers, on the field modeling of mechanical behavior of composites.

Table 2.1: Major research effort on the modeling aspects of particle reinforced composite

No.	Author	Procedure and Key findings
1.	S. B. Prabhu and L. Karunamoortthy [17]	• 2D microstructure based FEA. • Stir casting, ANSYS, Image conversion. • Predict micro level stress distribution. • Investigates influence of clustering & particle geometry on strength.
2.	B. P. Kumar and S. J. Babu [18]	• 2D microstructure based FEA. • Image conversion through wintopo software. • In Favor of Prabhu [1] results. • Achieved stress strain values and young's modulus.
3.	F. Ayari *et al.*[19]	• Comparative FEM study of 2D and 3D microstructure based model of ceramic reinforced composites. • Concludes 2D results closer to experimental results.
4.	G. G. Sozhamannan *et al.*[20]	• Divide his work into clustering and no clustering FEM analysis of 2D images. • Images taken from different processing conditions. • Concludes failure of PAMMC influenced through volume fraction, decohesion and volume fraction.
5.	M. Sambathkumar *et al.*[21]	• Worked on HMMC, SiC TiC reinforcement. • Used microstructure based approach. • Concludes increase in volume percentage reinforcement strength increases.
6.	N. Chawla and K. K. Chawla [22]	• Used 3D microstructure based approach and gives better understanding of material behavior. • 2D shows the anisotropy in deformation and thermal resistance stresses.
7.	Z. Peng and L Fuguo [23,26]	• Gets quantitatively consistent stress-strain behavior of 2D microstructure based model. • Strain rate and temperature plays minor role in affecting stress strain behavior. • Image processing method with help of MATLAB by measuring area and perimeter of reinforcements. • Establish FEM on the Matlab image processed microstructure to check the deformation of PAMMC.
8.	L.A. Dobrzanski *et al.*[24]	• Used fem for estimation of hardness of Mg alloys. • Modeled Rockwell hardness test with steel globule. • With the help of penetration depth and contact pressure estimate the hardness of composites.
9.	E. A. Diler and R. Ipek [25]	• Used central composite design method • Effects of matrix, particle size, reinforcement volume fraction on strength of Al-SiC composite was studied
10.	A Paknia *et al.*[27]	• Used 2D analysis of a patterned reinforcement having 4 different shape and 3 different concentration. • Applied tensile load and resulted the effect of different types of reinforcement shapes on stress- strain distribution inside the matrix.

2.3 Literature Review on the Mechanical Characterization of AMMC

In this section discussion is based on the metal matrix composite's mechanical properties. Improvements in mechanical properties are the basic requirements of the composites. Every composite are made on the basis to achieve certain properties. These properties are decided by the nature of work or implementation of the composite.

2.3.1 Hardness

Hardness defined as the resistance of a material to localized deformation or simply referred as resistance to indentation or scratch. The deformation can be in the form of indentation, cutting, scratching, elongation, bending. In case of ceramics, metals and utmost polymers deformation is considered as plastic deformation of the surface. For some elastomer and few polymers hardness defined as opposition for elastic deformation. Hardness can be measured through various techniques. Rockwell's, Brinell's and Vickers's are the most significant. Mixture composition plays vital role in approximation of hardness. Volume and reinforcement of individual constituent sets the hardness value which lies between the higher and lower value of constituent [3,5]. The reinforcement with Silicon Carbide (SiC), Alumina (Al_2O_3) and aluminized preferred for impart higher hardness. MMC having particle dispersed has higher hardness than other reinforcement [5]. SiC, TiC, Al_2O_3, WC and aluminide are better reinforcements for higher hardness. Ni and Cu coating increases the good quality interface characteristics. For increase in hardness to weight ratio, TiC dispersed in aluminum matrix but it influences the thermodynamic stability of composites [7].

The particle size also influences the hardness. **Howell** [6] **andVencl** [8] described the improvement in hardness by increases particle volume fraction. **Deuis** [11] reasoned that hardness of composites depends on the size and shape of reinforcement as well as interface bonding. **Subramanian** [28] concludes that weight percentage of SiC increases the hardness of the composites with increases in load bearing capacity of composites. Therefore, with increase in the filler content, hardness of composites increases.

2.3.2 Ultimate Tensile Strength

The mechanical properties of MMC depend upon the properties and structure of reinforcements. Various researchers found out that tensile strength of reinforced composites (SiC) is more than the unreinforced Aluminum. **Ramakrishnan** [29] concludes with the help

of mathematical formulation models concludes that addition of SiC in 6061 aluminum matrices helps to acquire 10-70% additional strength depends on volume fraction and particle size. Due to Al matrix, dislocation density close to matrix reinforcement interface increases and causes strengthening effect [30]. Tensile strength of MMC depends upon the stress transfer from metal matrix to reinforcement. Increase in reinforcement helps to bear more loads on strong SiC reinforcement. In composites, crack needs to propagate along matrix and reinforcement both due to strong matrix interface. Strengthening mechanism is described by **Reddy** [31]. He describes two possibilities for increase in strength, increase in reinforcement with smaller particle and other is formation of cluster or precipitates at the particle/ matrix interface. Small particle sizes have large surface area for transferring stress from matrix and nucleated voids are not blend easily.

2.3.3Compressive Strength, Flexural Strength and Toughness

The increases in yield stress are reported by authors in their researches [31-33]. The effects which affect the compressive properties of SiC due to matrix strength are discussed by **Ravi Kumarand Dwarkadasa** [33]. They reported that the yield strength increases with increases in volume percentage and age tempering but reduced in the condition of peak aged [33]. **Jayaram and Biswas[34]** investigated the rupture strength of SiC with different particle sizes and observed. Three point bend test did not show any tendency of increase in rupture strength with increase in volume percentage of reinforcement. But he reported that for the particle size between 25-65 micron meters of SiC having maximum rupture strength [34]. Also, **KalkaanliandYilmaz[35]** (2008) shows that 10% SiC reinforcement is best suited for getting maximum rupture strength. Below this percentage rupture strength reducing also reported in their studies [35]. In support of this **AlanemeandAluko[36]** reported Al 6063-SiC reinforced fracture toughness increased either by ageing treatment or by increasing the percentage of reinforcement [36].

Ceramic reinforced aluminum matrix has higher young's modulus, yield stress, ultimate tensile stress, breaking stress (fracture) and decrease in ductility reported in the many literature from which some of them are discussed above. The increments in flexural strength of metal composite were observed up to a definite percentage of reinforcement. Below that value of bending strength reduces. While in case of toughness increase in reinforcements affects the increase in toughness value.

2.3.4Micro and Nanoindentation Study

Babu and Kang [37, 38]showed an increase in interest of material characterization at the nano-metric scale using nano indentation. Generally it is done with the spherical or pyramidal indenters to know the hardness and modulus of elasticity of specimen. Measurement of the contact area indirectly is most distinctive feature of this test. In this author studied about the AMMC composites reinforced with 10vol% graphite and alumina produced by infiltration method. Nano indentations were performed at different locations of the sample of unreinforced Al and reinforced Al matrix. The nano indentation test with continuous stiffness measurement (CSM) reports increment in the value of hardness as compare to unreinforced alloy. He found out that the value of hardness and elastic modulus was more when indentation is performed near the reinforcement. He also concluded thatdepth varies due to presence of nano-pores and debonding between matrix and reinforcement causes the variation in modulus and hardness.

Pramanik *et al.*[39]paper's investigated the micro indentation of MMC with the aid of the FEM and stressed on the stress strain contours and possible particle fracture. For modeling author prepared a rectangular work piece of volume 20% particles of 18 micrometer in diameter. They assumed that particles perfectly bonded with matrix material. With the assumptions of quasi-static nanoindentation process and nature of indenter to be perfectly rigid simulation finite element modeling was performed. While loading, a downward increments of rigid body to induce indentation on specimen. The indentation is done on particle and between two particles. While indentation loading stage on particle, compressive stress is much higher to the matrix. This may be result in higher elastic modulus and hardness. In case of unloading there is highest stress generation occurs at the top surface of interface. But there is less tensile force generation at the interface. Whereas for the most part of the stress field are permanent at the end of loading causes change in the some of the parts. In case of indentation between two particles the stresses are fragmented between interface and particles. Very low amount of stress generated inside the particle. Author reports that the value of stress generated between the two particles is very low as compared to the stress generation in case of indenter on particle. Author concludes his detailed study with different cases with remarks about reinforcement causes in homogenous plastic deformation, changes in the direction and magnitude of stress in particle causes particle fracture. Author also reports that average residual stress at interface was in compressive nature.

Rodriguez *et al.* [40]formed a composite from Al-Li alloy 8090 reinforced with 15% SiC volume. After that nanoindentation test is performed on it with Berkovich indenter tip. The indentations were performed on different locations like ceramic particle, matrix and unreinforced alloy. After indentation test two dimensional finite element modeling analysis were analyzed in ANSYS software. With some certain assumptions for ease of modeling like frictionless contact between matrix and specimen, conical tip with same semi vertical angle 70.3 and radius tip of 100nm, model is analyzed with same constraints as actual test load applied on it. In the end numerical model was checked by comparing the results of experimental and simulation results. Same procedure is followed in case of unreinforced alloy to get the load displacement curve. In conclusion of their work Rodriguez et al. concluded that results obtained from both, the experiment and simulation holds a good agreement and suggested to consider it in micromechanical models.

Waigh and Fathy [41] provided a non-destructive method to know the basic mechanical material properties with the help of FEM. For this, the authors prepared nano-composites of Al-Al_2O_3 by powder metallurgical method. Mechanical behavior of composites was investigated with the tensile test. To obtain the properties at the nano level indentation experiment performed on the polished sample of composites. The average of the five values of indentation curves was used as simulation of test in FEM. The finite element model was employed for simulation which was based on the ISO 14577 standards. With conical tip of radius 150-200 nm and axis- symmetric condition, mesh was created. The area of interest in this simulation is the contact region of tip and sample. A condition of contact pair with no friction condition was applied on it. Tensile test properties were used to define the material mechanical values. Constraints on the indenter were same as actual conditions. Author reported that there was bad agreement between sharp tip indenter displacements with compare to actual experiment. But in case of rounded tip there was good agreement which holds the simulation and experiment values close together. Author concludes that there was negligible change in hardness values of experiment and simulation results and finite element load displacement curve was consistent with nanoindentation results.

2.4 Research Gap

Literature review is done extensively on the modeling of mechanical behavior and mechanical characterization of AMMC along with the emerging trends of research involving composites. A lot of effort has been done to produce and achieve desired properties by

mixing or reinforcing it with the different types of reinforcements. Since alloys are easily stable and more resistant to changes in environments conditions, they are more preferable to the pure metals in the production of composites. Aluminum is one of the most favorable for matrix element due to its low weight, easily abundance and smooth handling. To improve its hardness, wear behavior various kinds of particles are reinforced within the base metal/alloy. But to test the composite materials, there are conventional methods which are destructive, tedious and time consuming.

In recent years with the developments of analysis software's to estimate the safety of material, researchers are trying to simulate the most of the tests of the composites on the computes. With the development of high speed computer with less computational time and multipurpose ability it is classified as a type of non- destructive test. Various mathematical and hypothetical models already are presented by many of the researchers to establish good agreements between the experimental and simulation results. However, works which involves mathematical modeling is tedious and time consuming task. Some researchers used image processing methods to investigate the mechanical behavior of composites with the help of finite element analysis software's.

Based on the literature review on worldwide research in the relevant area following research gaps are identified.

- There is very limited work found in the literature which determines mechanical properties of particle reinforced MMC using numerical or analytical method by taking account of the reinforcement's actual size and shape. Mostof the researches involved with modeling of mechanical behavior used predefined shape andsize of reinforcement in the matrixto predict the deformation behavior of composite.
- Very few researchers made attempt to validate the mechanical and material properties of the fabricated composites with the simulated properties for actual conditions.
- Limited literature is available on the works which experimentally investigated the localized mechanical properties such as micro and nano hardness of composite which are subsequently used as the material properties in the image based and FE modeling work to predict the mechanical behavior of the same composite.
- Also, most of the researchers took interest in the gross effect of reinforcement by characterizing the mechanical properties. Theoretical investigation for the effects of reinforcement in the random morphology on the deformation behavior of the composite are least explored.

Chapter 3

Research Objectives, Materials and Methodology

3.1 Research Objective

The objectives of the proposed work are:

1. To fabricate and characterize Aluminum Metal Matrix Composites
2. To obtain the nano and micro hardness and young's modulus of composites
3. Generation of CAD model from microstructure with image processing technique.
4. Simulation of nanoindentation process and comparing it with experimental results.
5. Simulation of stress-strain distribution under tensile loading and to compare simulation results with the experiment results.

3.2 Planned Methodology

To achieve the desired research objectives following step by step procedure is followed.

1. Fabrication of composite.
2. Experimental investigation of mechanical properties of composite.
3. Obtaining the microstructure of randomly distributed particle.
4. Image generation of specimen using image processing software.
5. Design a CAD model on the basis of image obtained from image processing software.
6. Implement the individual property of matrix and reinforcement material to CAD model.
7. Applying constraint on CAD model and obtaining deformation behavior.
8. Validation of the models by comparing experimental and predicted values of deformation.

The flow chart of planned work of experimental and microstructural investigation is shown in Figure 3.1.

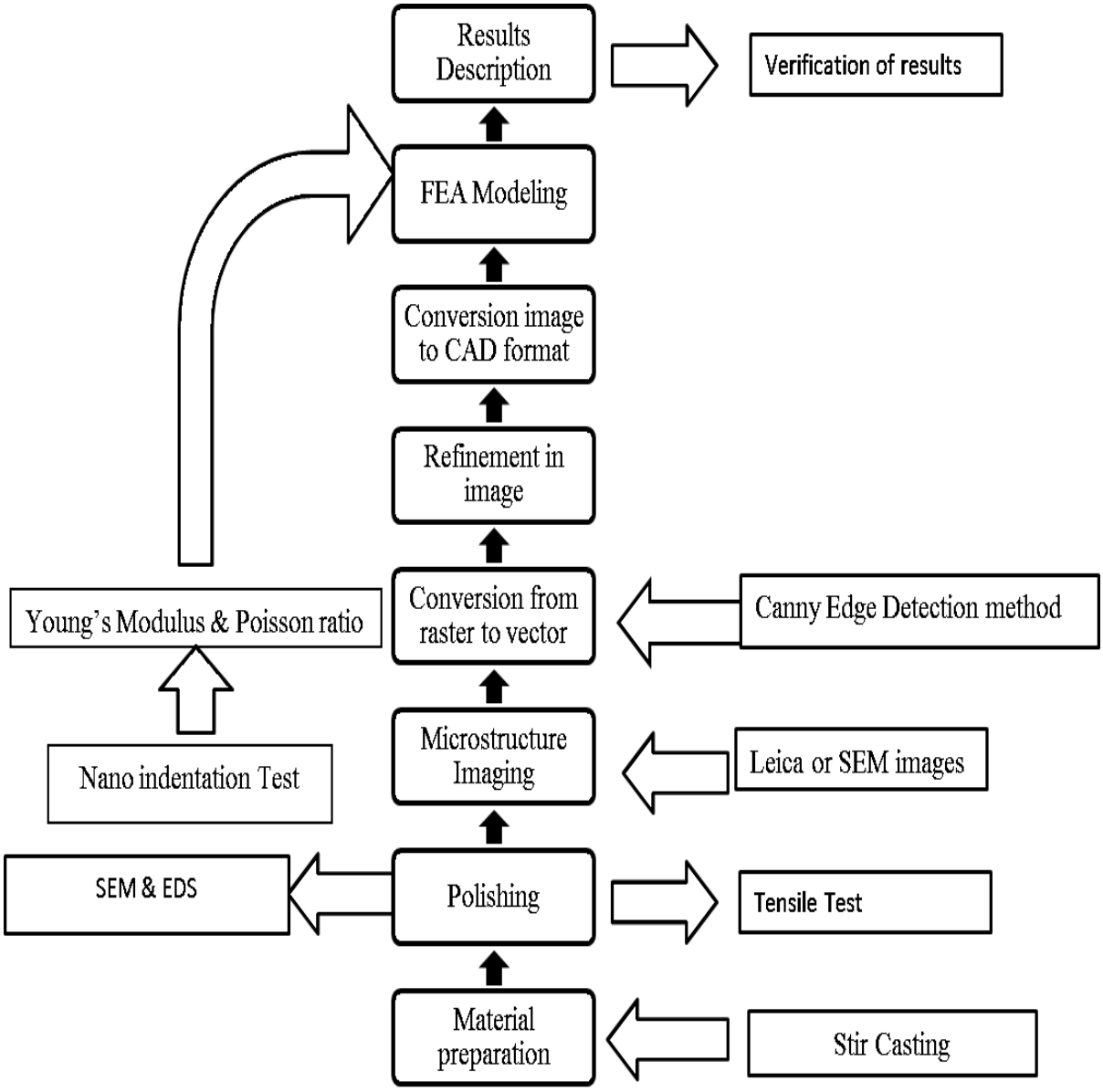

Figure 3.1: Bottom- up approach for planned work

3.3 Methodology

This section of the thesis describes the details of the instrumentations used, sample preparations for different experiments, description of software and analysis tools.

3.3.1 Materials

In the present study well known Aluminum 6061 alloy is used as the matrix material and Silicon Carbide as reinforcement. There are sufficient literatures provided that ensures the improvement in mechanical properties of composite by adding silicon carbide as reinforcement to aluminum. Aluminum 6061 was obtained in the form of tubes. The compositional description of Aluminum alloy was shown below in the Table 3.1.

Table 3.1:Chemical composition of Al6061 by weight percentage [42]

Chemical percentage	Si	Fe	Cu	MN	Mg	Cr	Zn	Ti	Al
Al 6061	0.4-0.8	Max. 0.7	0.15-0.4	Max. 0.15	0.8-0.12	0.04-0.35	Max. 0.25	Max. 0.15	Balance

On the other hand, reinforcement SiC is obtained through Central Drug House, Ludhiana of 300 mesh size which gives optimum results.

3.3.2 Method of Manufacturing AMMC

With the variety of manufacturing process provides in this country for discontinuous MMC, stir casting is accepts as a particularly promising route due to its flexibility, simplicity and applicability to large quantity production. The stir casting is the most cost effective with uniform distribution, method of liquid state fabrication. It minimizes final cost of the product and allows very large sized components to be produced. AMMCs used for the present study is fabricated by Stir casting.

A pre weighted quantity of 6061 Al alloy were taken in a graphite crucible and melted it until red hot liquid state in an electric furnace. The temperature rose up to 850°C with slow increment in their temperature. While melting the matrix material, reinforcement material is preheated in the microwave oven at a temperature of 450°C to drive off the moisture. The molten metal was stirred through with the help of 3 blade stirrer to create vortex at speed of

630rpm. For creation and maintaining proper distribution of reinforcement in the matrix vortex is best known approach. With the formation of vortex during stirring preheated reinforce material is added into it with the continuous rate of 20-30gram per minute. The stirring was performed 5 minute more after adding the particle into molten metal for appropriate bonding and homogenous distribution. A metal mould which is coated with graphite is used in which molten metal poured and solidifies at room temperature.Figure 3.2 shows the different parts of stir casting and Figure3.4 shows the cast Al- 10wt% SiC sample.

Figure 3.2: Stir casting setup (a) Furnace with motor and temperature controller (b) Graphite crucible, (c) Muffle furnace [Photo Courtesy: Central Workshop at Thapar University]

Figure 3.3: Cast sample of Al- SiC composite

3.3.3 Microstructure Characterization

Scanning Electron Microscopy: SEM is used for examining of chemical composition and microstructures with Energy Dispersive X- Ray spectroscopy. With the help of high magnification lens and electron beam surface region of the specimen's surface examined. The lens produces high resolution images of the surface and electron combines with the atom of sample to show the microstructural data. Figure 3.3 shows the Model No.: JEOL JSM-6510LV available in the SAI Labs at Thapar University, Patiala as shown in the Figure 3.4.

Figure 3.4: Setup of SEM and EDS[Photo Courtesy: SAI Labs at Thapar University]

X-Ray Diffraction(XRD)*:*The microstructure of composites with different compositions and elements are determined by the XRD technique. It is the one of the most used techniques to classify composites structures. In this technique X- Rays is being produced when the high speed electron beam strikes to a specimen. The electrons are travel through hot tungsten filament to high accelerating voltage acting as a cathode. Low temperature copper block having the specimen is act as anode. The composites structures identified by continuously monitoring the counting the intensity of reflections from the specimen surface and position.

When the electron beam strikes on the specimen surface the atomic planes of a crystal causes interference with one another while leaving the crystal. The whole phenomena of XRD based on the Bragg's Diffraction law Eq. (3.1) which states that

$$2dsin\Theta = n\lambda \qquad (3.1)$$

Where, d= distance between lattice planes

Θ= angle between diffraction waves

n= numeric constant known as order of diffracted beam

λ= wavelength of beam

Figure 3.5: X-ray Diffractometer[Photo Courtesy: SAI Labs at Thapar University]

3.3.4 Microhardness

The hardness determination of composites gives the micro level effects of particulate reinforcement on the alloy matrix. The samples were well polished until mirror image surface not obtained before microhardness testing. The Vicker hardness testing machine Mitutoyo Model number MVK_H0 as shown in the Figure 3.7 made in Madras, India had a diamond indenter tip of radius 250nm. It is also had 40x and 10x lens for proper location and indentations. Vicker Hardness (H_V) calculated through with the help of following Equation (3.2).

$$H_V = 1.854 \frac{F}{d_{mean}^2} \quad (3.2)$$

Where F= load in kgf, d_{mean}= Arithmetic mean of the two diagonal, d_1 and d_2 in mm.

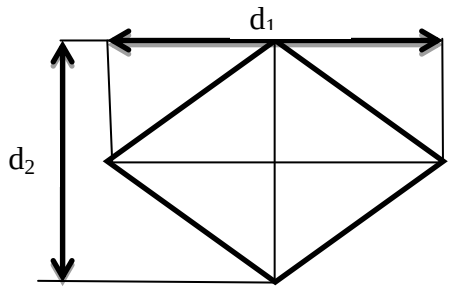

Figure 3.6: Microindentation diagonal measurement

Figure 3.7:Mitutoyo microhardness tester[Photo Courtesy Advance Measurement Lab, Thapar University]

During indentation the procedure completes in three stages i.e. loading in which loads applied on the location causes elastic deformation, dwell period where indenter dwells with the surface of the specimen and unloading in which load removes from the specimen. After unloading there is some permanent deformation on the surface of the specimen which will be seen through lens in the form of indenter's shape.

3.3.5 Nanoindentation

The nano indentation method is one of the most trending methods to know the material properties at the least micron level. Its indent is in the range of nanometers. It is commonly known as depth sensing indentation due to estimation of indentation depth at nano meter scale.

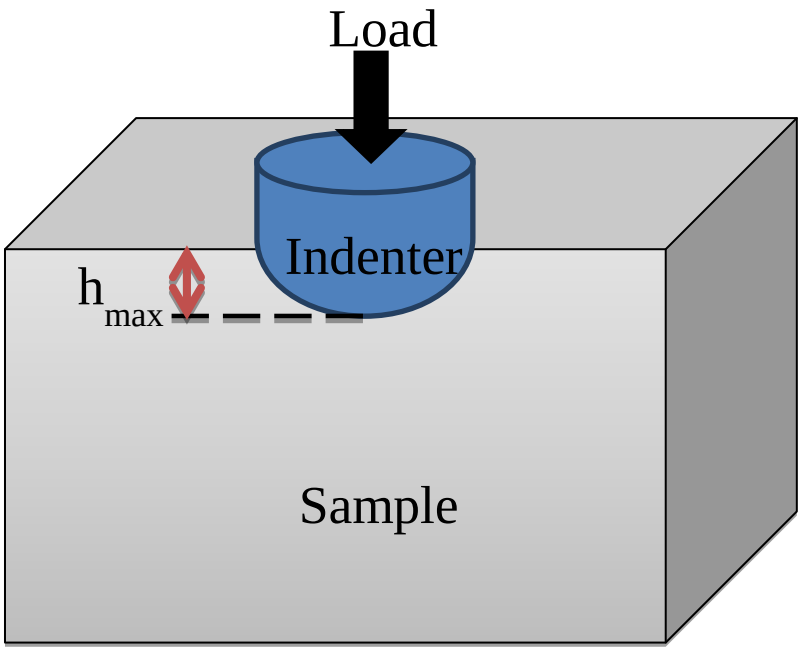

Figure 3.8: Schematic representation of indentation process

Indentation is a process defines as process in which a specimen of examined material is kept under certain known load until an impression is made on it. With the help of depth sensing techniques area of indentation and depth of indentation is calculated which eventually give hardness of the material. Figure 3.6 shows the basic setup of indentation process. But there is difference in nano-indentation and other hardness estimation methods. While performing test of specification tip shape and size with known material properties indenting a specimen at very low load using a high precision instrument. During indentation with the help of sensors simultaneously records the load and penetration depth. These load and depth

penetration of loading and unloading values helps to evaluate the mechanical properties of specimen with significant data analysis.

Sneddon (1965) studied the deformation of an elastic half space with the help of a rigid, axisymmetric punch of arbitrary profile. In their result he established a relationship between the depth of penetration and the load applied by the punch. There are some assumptions which are made while deriving the analytical solutions i.e. infinite half space of specimen, ideal geometry of known parameters and material properties elastic and incompressible of indenter [43]. In 1992 Oliver and Pharr proposed an improved method relating the depth of indentation with the indenter topology with the goal to establish the contact area of specimen and indenter's peak load. Subsequently, they proposed an approximate calculation in the form of hardness and elastic modulus from the load – displacement data [44]. Significant effort in nano-indentation helps to produce the evolution of FEM-based algorithms simulating the process to determine Elasticity Young's modulus and hardness of material [45]. All the above mentioned works, have contributed to the establishment of ISO 14577 which is adopted as the standard test for nanoindentation.

This test includes three stages i.e. loading, dwell time and unloading. Figure 3.9 shows typical Nano indent load vs penetration depth. The image described on the basis of the theory produced by the Oliver and Pharr method as the figure shows with increase in the load penetration depth also increases in case of loading. The highest values of penetration depth i.e. h_m and includes elastic and plastic deformation. After loading there is dwell period in which indenter abide along with specimen. In the end, unloading starts in which there is gradual decrease in applied load.

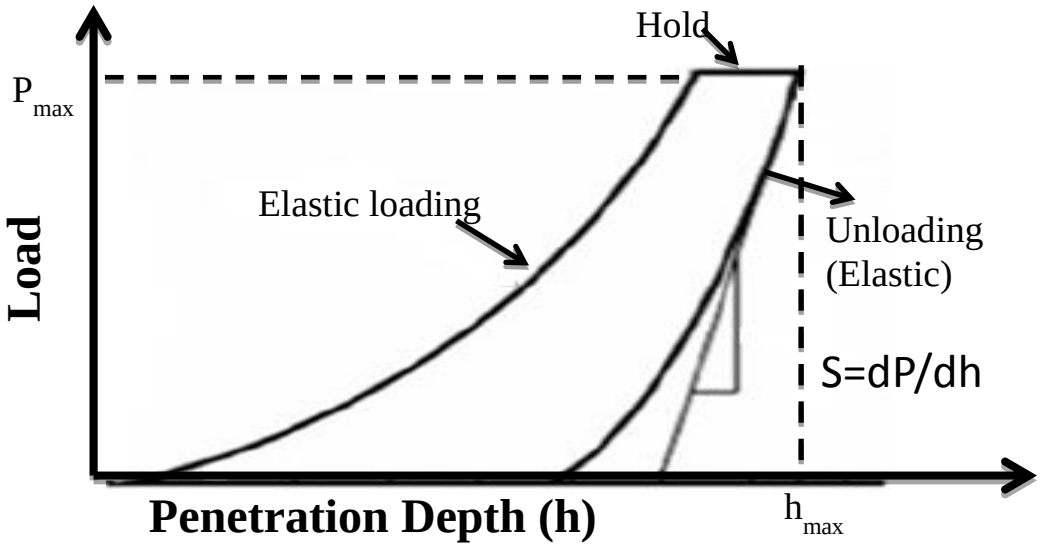

Figure 3.9: Various stages during nanoindentation process

The point at which indentation depth becomes zero is final indentation depth h_f. After performing this test there is permanent deformation mark on the specimen. Stiffness is defines as the slope of unloading curve. In other words it is the ratio of change in load with change in penetration during the first moment of unloading. The contact depth and cross section area is to taken to calculate the hardness.

According to Oliver and Pharr method, contact depth is obtained as:

$$h_c = h_m - \delta F_m/S \qquad (3.3)$$

Where h_c= contact penetration depth

h_m = maximum penetration depth

F_m= Maximum Force

S= Stiffness,

With the help of knowing contact depth, cross section area A_p is calculated. The Vicker hardness HV is calculated from the developed area A_d

$$HV = F_m/A_d \qquad (3.4)$$

Whereas instrument hardness is calculated from peak load F_m and projected area A_p of contact as:

$$HV_{IT} = F_m/A_p \qquad (3.5)$$

Difference in instrument and Vicker hardness of material resides in the area of contact and developed area. With the help of stiffness and contact area reduced elasticity is obtained. Reduced elasticity id used to account for the fact that elastic displacement occurs in both indenter and specimen. This reduced modulus helps to find the instrumented modulus of elasticity E_{IT} by the relation:

$$E_{IT} = \frac{(1-v^2)}{\frac{1}{E_{IT}} - \frac{1-v_i^2}{E_i}} \qquad (3.6)$$

Where, E_i= Indenter Young's Modulus of Elasticity

v_i = Indenter's Poisson's Ratio

E_{IT}= Instrumented Young's Modulus

The diamond indenter's properties which used for indentation are as follows- Indenter Young's Modulus of elasticity (E_i) is 1140GPa and Poisson's ratio is 0.07. The nano indentation test was performed by TI950 series Hysitron Tribo Nanoindenter using a berkovich indenter which is shown in Figure 3.8. The TI 950 is decked with Hysitron's patented 3 plate capacitive transducer technology. The system enables with force noise floor,

ultra-fast feedback and user defined data acquisition rates up to 30 KHz. It also combines with in-situ imaging which facilitates unmatched precision in test placement and data accuracy. All feedback control functionalities performed the combination of Dedicated Signal Processor (DSP) and Field Programmable Gate Array (FGPA) embedded control system. To provide environmental isolation custom enclosure helps to avert the effects of temperature, noise, air currents and vibrations. Figure 3.10 shows the nanoindentation machine situated in the Biomechanical Characterization Lab at IIT, Ropar.

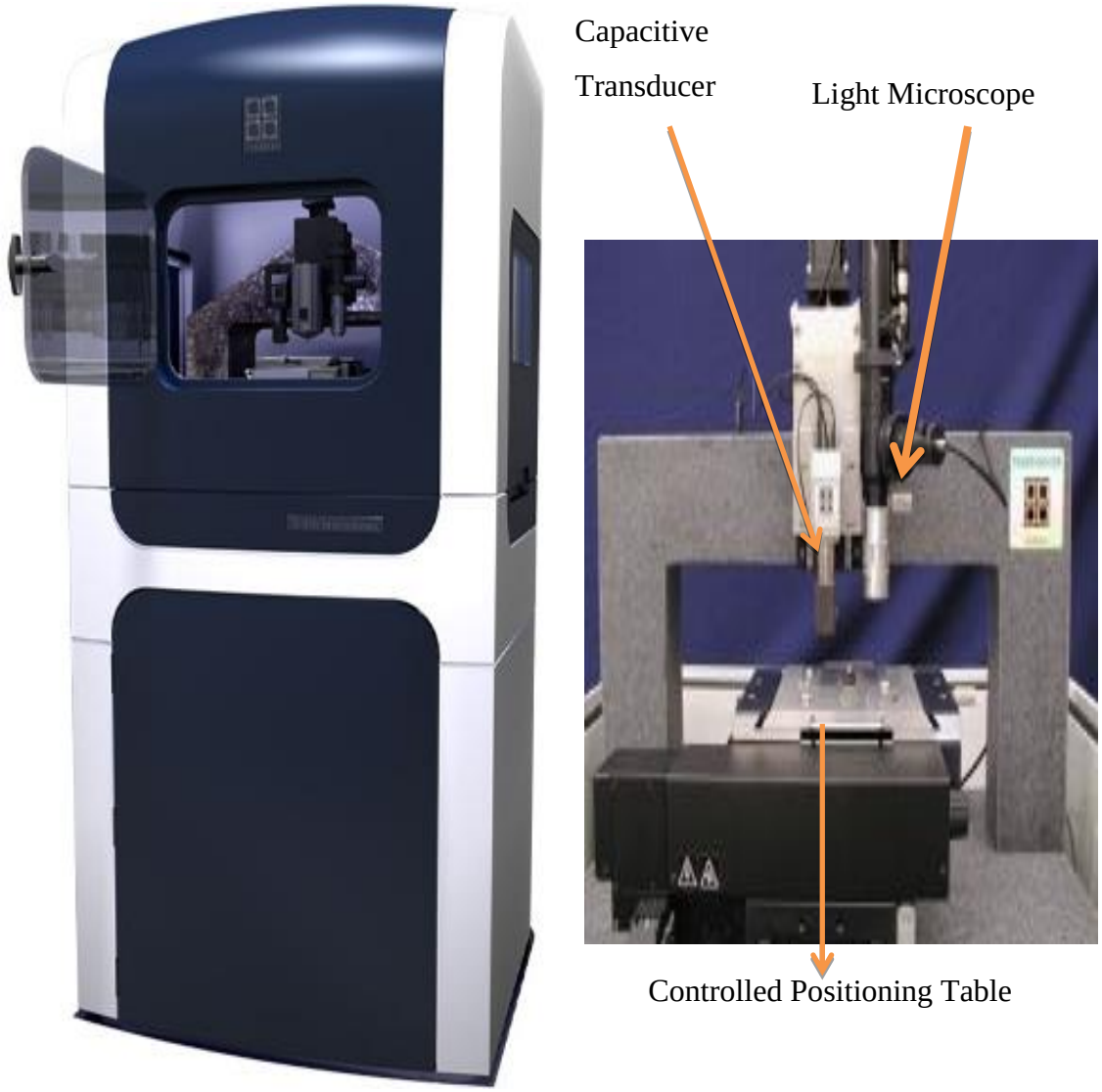

Figure 3.10: Hysitron Ti 950 Nanoindentation machine and indentation setup

3.3.6 Software forFEA and Image Processing

Student licensed version of ANSYS 17.1 was used for conducting the finite element simulation in this study. The software has the ability to solve complexity of nonlinear problem. The main reason for choosing ANSYS over other software is its ability to employ gap elements in case of contact problems. With this, control over load steps /sub steps provide data occurred at various points or time. Finite element simulation of the indentation with axisymmetric half space model was developed to reduce the computational time.

Wintopo is image conversion software which convert bitmap image to CAD format. In this research freeware version is used. This software is used for high quality images TIF, JPG, PNG, BMP files to as required CAD and CNC applications. This software is a product of SoftSoft Limited registered in England. In this software one touch vectorisation method is used to convert image into raster format. Canny edge detection method was used to extract raster data from the image. In Wintopo processing of image done through two stage of vectorisation employed. One is thinning of raster image to single pixel width lines and other is extraction of real vectors from pixel lines. Thinning is method which converts image into lines of pixels. Canny edge methods works on the edges of object which is beneficial for images having solid regions. These solid regions only need to vectorise the outlines. This method also helps to find boundaries of poorly defined objects.

Chapter 4

Results and Discussion

4.1 Introduction

This chapter deals with the detailed results and discussion on the characterizations of the fabricated composites as well as the deformation behavior through nanoindentation, micro-indentation, image processing and FEM modeling. SEM micrographs and the optical macrographs are also presented.

4.2 Microstructural Characterization of Powders and Composites

Al- SiC MMC samples of 5cm x5cm x 5cm sizes were cut from the cast blocks for polishing. First of all, the samples were leveled with the help of filer. The polishing of samples is done through emery papers with grit sizes ranging from 600-2000 grit size on disc polisher. To achieve nano polished surface diamond paste is applied on the surface and rubbed it on velvet cloth for 2-5 minutes. The continuous monitoring of the surfaces of each sample while polishing is done through an inverted optical microscope (LEICA). Figs. 4.1 and 4.2 show the SEM micrograph and EDS of SiC used as the reinforcement for the composite.

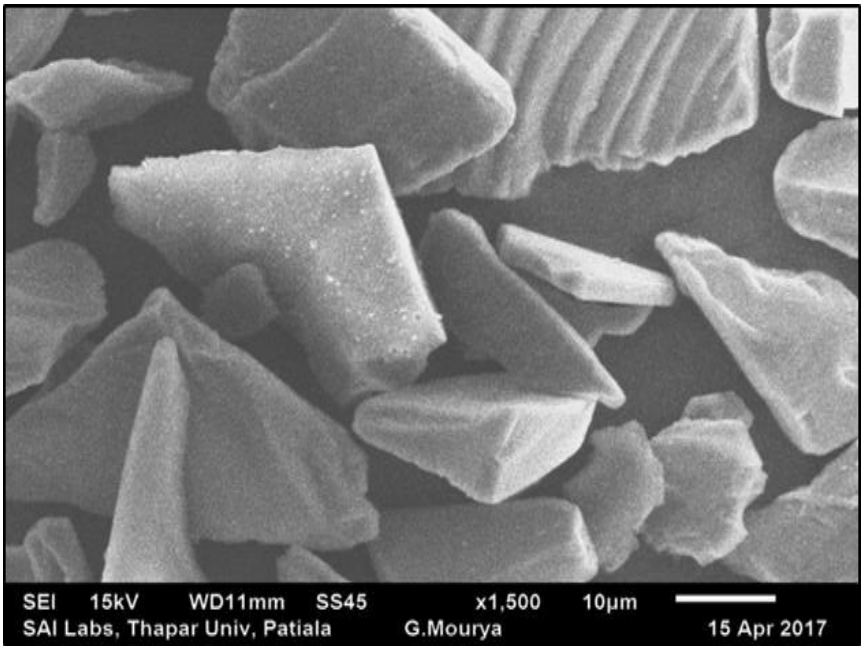

Figure 4.1: SEM image of as received SiC powder

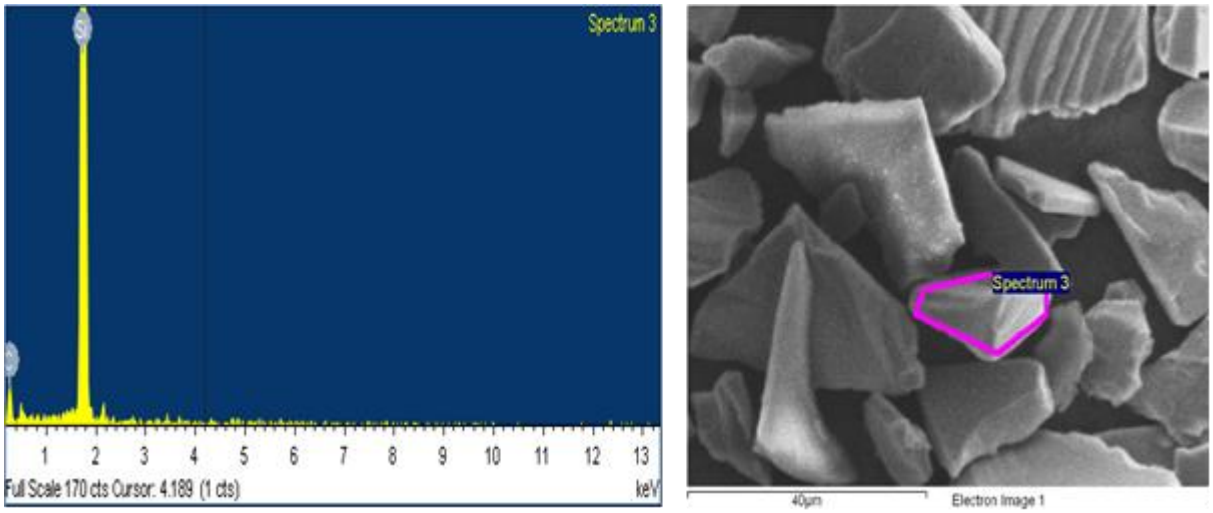

Figure 4.2: EDS of SiC powder

The optical micrographs of particulate reinforced MMCs are shown in Figure 4.3, Figure 4.4, and Figure 4.5. The homogenous and uniform particle distribution is observed from the micrographs. The main requisite for best performance of composites is homogenous distribution of the reinforcements into the matrix. It is clear from the image that dendritic growth is subdued due to presence of reinforcements which in time gives better mechanical properties.The optical micrographs were taken at different magnification level for better investigation of particle bonding and distribution.

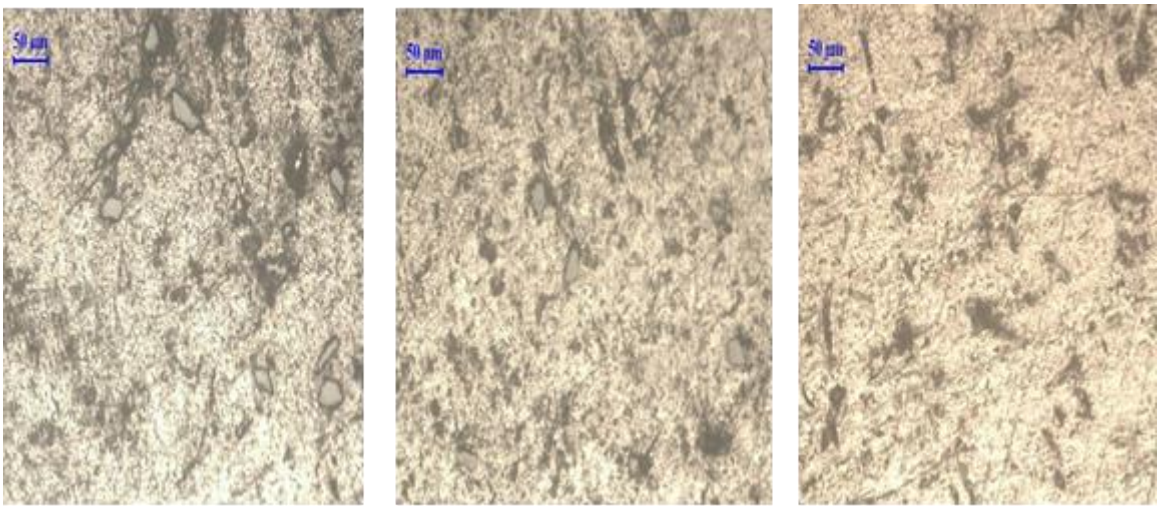

Figure 4.3: Optical micrographs of the Al- SiC composite showing uniform distributions

The composite's optical micrograph at various magnification scales describes the distribution and particle bonding. The optical micrographs shown in Figure 4.3 indicate that there is the homogenous distribution of reinforced particles in alloy matrix. It is achieved due

to high shear rate generation due to stirring of the slurry and stirring also resists the setting of particles. In case of matrix, dendrites are also observed but it is fragmented form. Fragmentation of dendrites describes by the shearing of previous dendrites by stirring. During particle additions there is a temperature difference between the particles and melt causing preferential solidification. At higher magnification finely distributed particles are clearly visible, as shown in Figure 4.4. However, in some of the areas particle clustering is also observed. This may be due to the fact that the fine particles are advancing Solid- Liquid interface during solidification. At higher magnification it is clearly seen that there is smooth interface between matrix and particle.

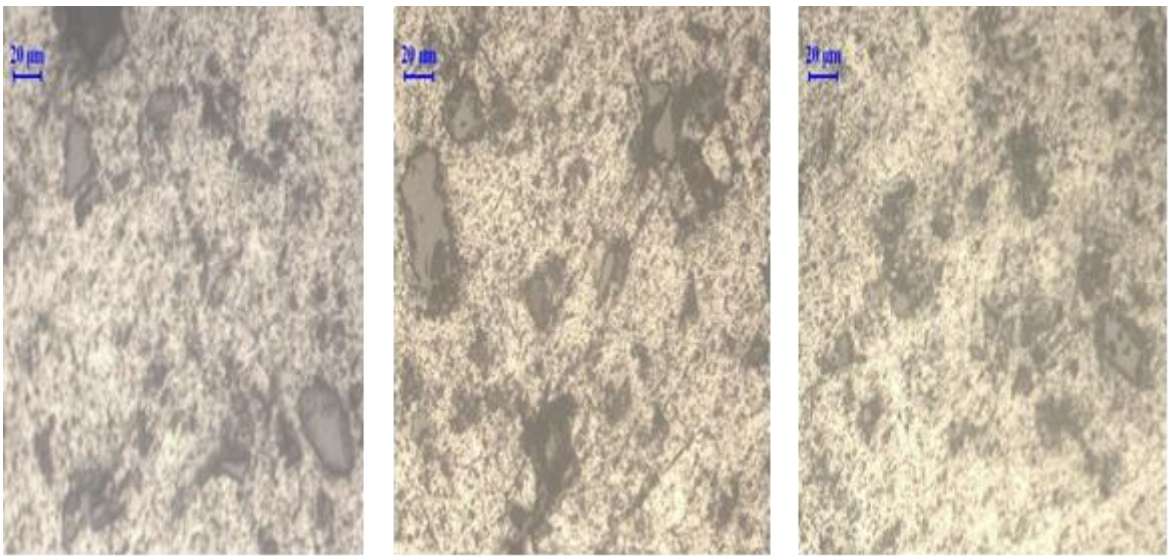

Figure 4.4: Optical micrographs of fabricated composites at 20X magnification

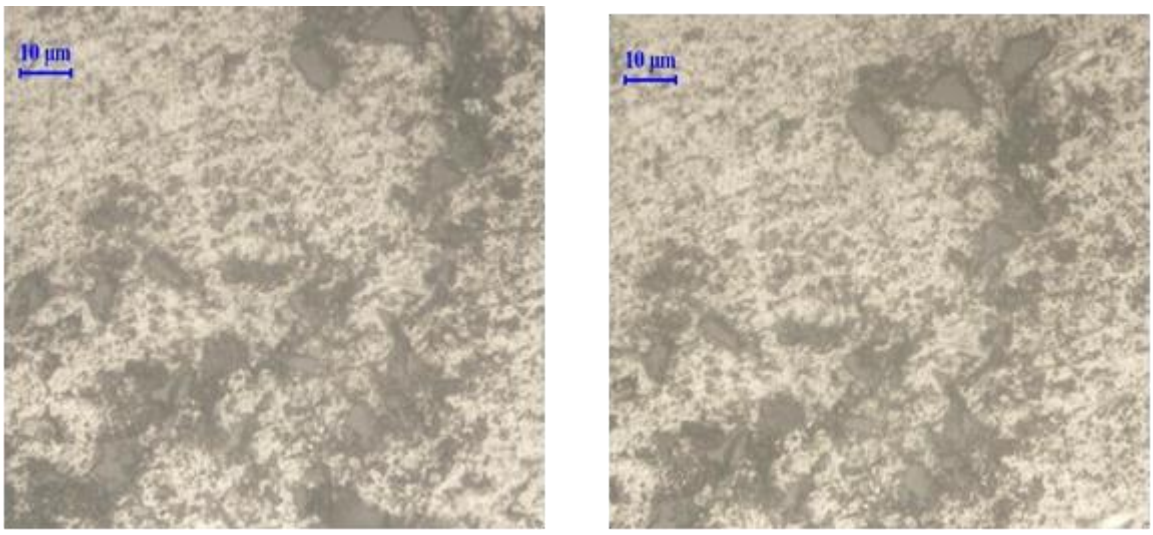

Figure 4.5: Optical micrographs of fabricated composites at 50X magnification

Similarly, the SEM images Fig. 4.6 of Al-SiC(10 wt %) composite clearly showed the proper mixing and dispersion of reinforcement throughout the material and there is mutual insolubility between reinforced SiC and matrix of aluminum material. At some places few voids also seen due to removal of reinforced particles at the time of preparation of sample.

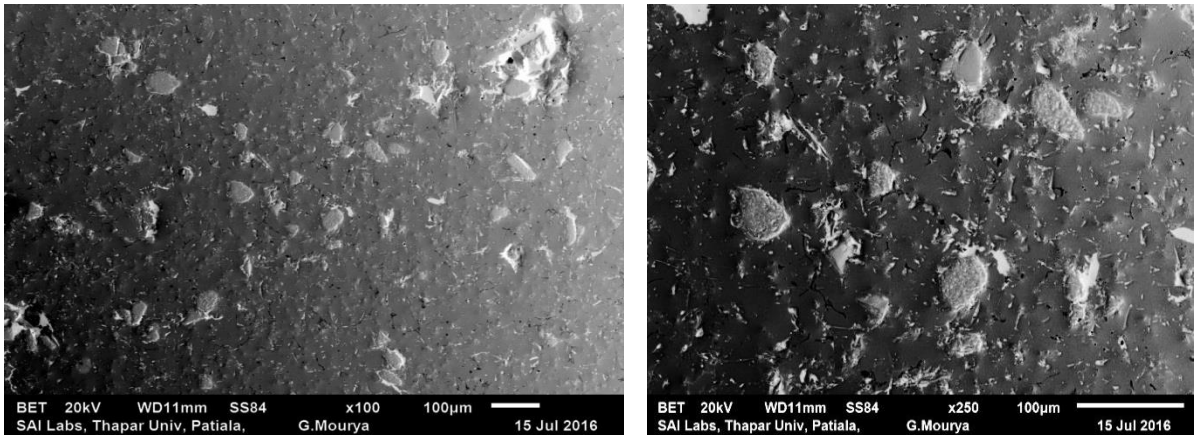

Figure 4.6: SEM image of Al-SiCcomposite casting

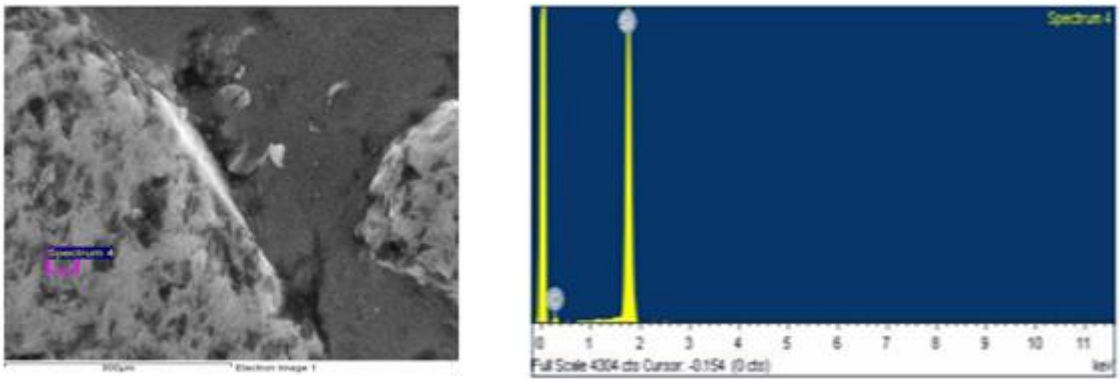

Figure 4.7: EDS of Al- SiC at reinforced SiC particle

Figure 4.7 shows the Energy Dispersive X- Ray Spectroscopy (EDS) of the prepared Al-10%wt. SiC composite. Element compositions obtained from the EDS are also shown in Table 4.1 which describes the presence of Silicon and Carbon percentage in composite.

Table 4.1: EDS composition of Al- SiC at reinforced SiC particle

Element	**Weight%**	**Atomic%**
C K	35.62	56.40
Si K	64.38	43.60
Totals	100	

4.3 XRD Analysis

Sample preparation for XRD is same as SEM but the height of the sample is reduced (less than 5 mm). Polishing of the surface is done till the mirror finishing was not obtained by different grit size emery papers.

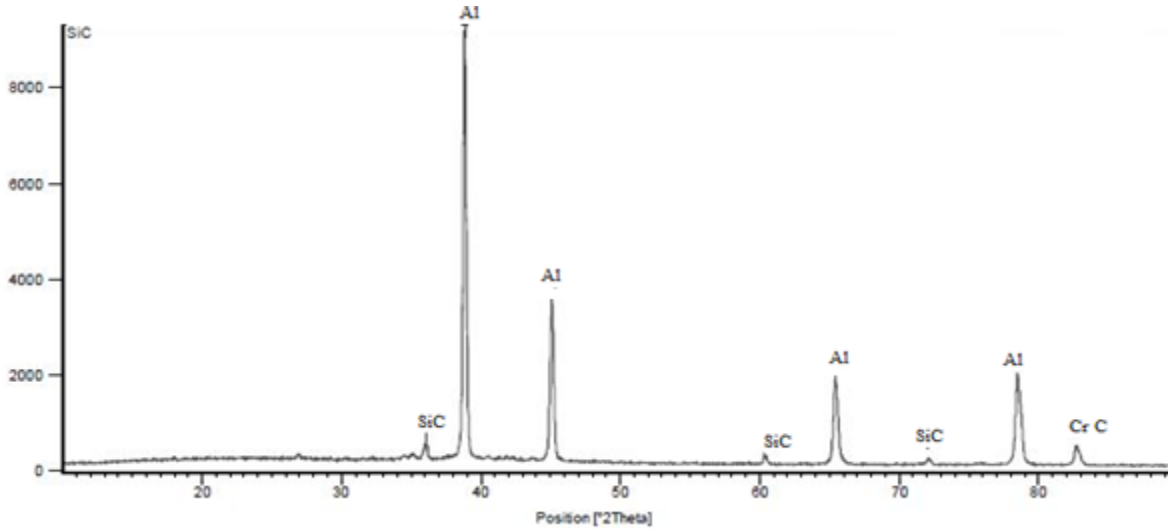

Figure 4.8: XRD Spectrum for Al-SiC

In the figure 4.8 various peaks are observed from position of 30-85°. Aluminum (Al) clearly dominated the whole XRD pattern. XRD analysis clearly shows the presence of Silicon carbide in the aluminum matrix. Some negligible peaks for oxides and chromium carbides are also observed which may be due to decomposition at higher temperature in casting. Since, chromium is present in the base metal so it forms chromium carbide. The highest peak observed at the angle of 39° which is identified as Aluminum (matrix material) from the reference pattern. The second highest peak observed at the angle of 45° of reinforced silicon carbide in the form of moissanite. It is shown clearly that there is no major interaction between base metal aluminum and reinforced silicon carbide. Also there is no presence of significant oxidation as seen in the XRD pattern.

4.4 Hardness

To obtain the microhardness values, microhardness tester is used. To obtain the clear and visible indented images, the samples were suitably polished. The measurement of micro hardness is done at different locations of the composite. The micro hardness measurement is

done near the interface of the matrix and the particle to avoid the artifacts involved with the pure particle indentation or matrix indentation which is far away from the particle boundary. Five readings per sample have been taken from the hardness tester and an average value is calculated for the hardness of composite. The deformed region is too small when indented on the reinforced SiC particles due its high hardness whereas as we move far away from the particle boundary towards the matrix the influence of reinforcement gets diminishes, hardness started decreasing and the value reaches towards the hardness of pure aluminum.Figure 4.9 shows the images of the indentation obtained from the microhardness tester on cast aluminum sample and Al-SiC composite sample.

Figure 4.9: Indentation images of (a) cast aluminum and (b) composite

The average value of five readings per sample has been taken via hardness testing machine at the load of 100gf and 20 seconds dwell time period. The hardness of the cast aluminum and Al- SiC composite is shown in the following Table 4.2. The average value of the hardness is found to be 71.16 of cast aluminum and 103.4 of reinforced silicon carbide aluminum composites. The measured value of the composites and cast aluminum holds good in agreement with the previous reported values from the various researchers [3-5, 28].

Table 4.2: Microhardness of cast aluminum and Al- SiC composite

Specimen	Test 1	Test 2	Test 3	Test 4	Test 5	Average
Cast aluminum	71.78	72.05	68.62	72.80	70.54	71.16
Al- SiC composite	101.38	104.88	102.36	103.54	102.69	103.04

4.5 Nanoindentation Method

Sample Preparations: A cuboid specimen of 10x10x5 mm was prepared from pure aluminum and Al-SiC composite. The surface of both the samples was mirror polished. The purpose to apply diamond paste is to obtain the nano finished surface because at the time of indentation roughness is the main affecting parameter which affects the results directly. The sample specimen's roughness is maintained less than 100 nm which is desirable to get good results. At the time of experimentation sample was mounted on the steel disc with the help of strong adhesion feviquick. It prevents sample's movement and damage during experimentation.

Nanoindentation Experimentation: The load-penetration graphs obtained from nanoindentation test are shown in Figure 4.10& 4.11. In case of loading, load increases from zero to highest value in sub steps of small increments. With the increase in the load, depth of penetration increases simultaneously. Accordingly, the graph values increases with respect to each other until dwell time starts. Following dwell time, unloading cause's gradual removal of loading from the specimen i.e. back to zero. But due to plastic deformation it does not follow the same path. Permanent indentation marks takes place due to which certain depth of penetration is maintained in the end. For all the tests standard 0-1000 μN load is applied on the specimen who generates 2400 points.The parameters and values obtained are shown in Table 4.3.

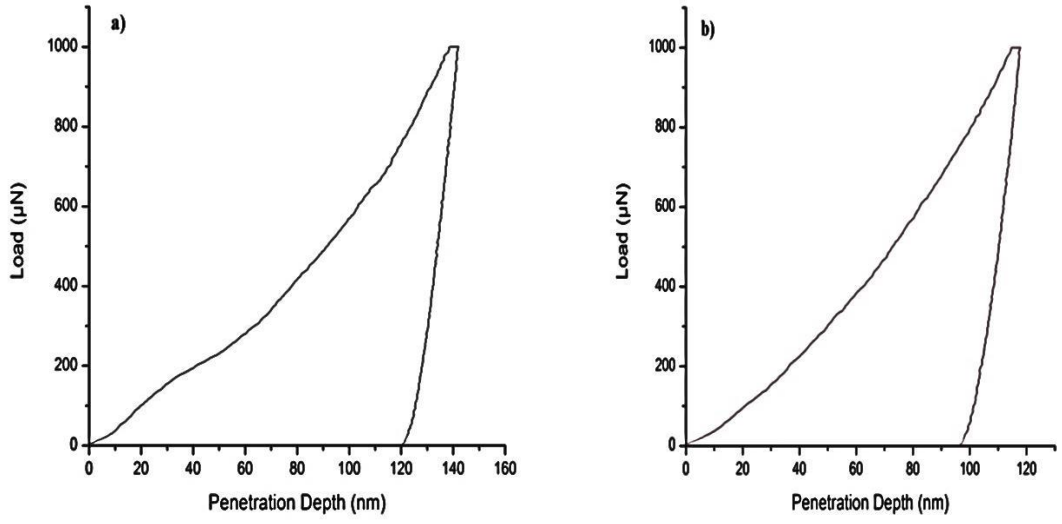

Figure 4.10: Load vs Penetration depth of (a) pure aluminum and (b) composite

The graph shown in the Figure 4.10(a) is of pure aluminum sample between loads versus depth of penetration. As we can see in the graph, the value of depth of penetration increases linearly with the applied load in early stage of loading. This is due to the reason of direct interaction between surface and indenter's tip which starts the elastic deformation. Hence deformation is linearly elastic until depth of penetration reaches 60 nm. After that there is slight change in the slope of curve is seen. According to theory of indentation after elastic deformation material goes to the elastic- plastic phase with further increase in load. Due to this reason indentation impression impinges on to the surface and causes permanent deformation on the surface of sample [46]. This phenomenon is represented by a slight change in the curvature of the graph. After 60 nm depth of penetration elastic- plastic loading starts where indent of the indenter causes permanent deformation on the surface. Material deform from this point onwards are permanently deformed and not able to regain its original shape. This plastic deformation occurs till the maximum load is applied i.e. 1000 μN and leaves a residual impression on the surface of the sample. At maximum load maximum depth of penetration is attained.

The depth of penetration and area of deformation is calculated by the optical methods based on the principles described in nanoindentation methodology. Penetration depth and indenter's geometry help to get indirect measurements of the hardness of the sample [44]. When unloading starts due to elasticity material tries to regain its previous shape but plastic deformation restricts it. Due to this restriction the graph must be a straight line till the applied load reaches to zero. But there is little extent by which material tries to recovers its shape due to relaxation of elastic strain within the material. Determination of elastic modulus and hardness from the nano indentation displacement curve are already described in previous chapter.

In case of Al-10% wt. SiC composite sample load versus displacement graph shown in Figure 4.10(b), same phenomena of elastic and elastic- plastic deformation occurred in loading curve as described above. For the nanoindentation characterization of the composite indentation is carried out near the interface of the particle-matrix boundary of the uniformly distributed zone of composite (now onwards the values obtained in these regions will be taken as the representative values for the composite). The curve starts with elastic deformation with constant slope between load and depth of penetration. As the load increases, depth of penetration increases and deformation at the surface also increases. At 40mm depth of penetration there is point where elastic loading sudden change in the

curvature of the loading graph was seen. This is due to the fact that with increment in load, tendency of material to regain its original decreases. The main reason behind this is the decrease in ductility of the composite as compared to metal alloy due to addition of hard ceramic reinforcement. Further increment in load causes change in applied loading effect from elastic loading to plastic loading which causes permanent deformation. This change is shown in graph at the point where curvature of the graph changes. This curvature remains constant till the maximum applied load has not been attained. In unloading of the indenter similar pattern as metal was shown by composite in form of elastic unloading. The ratio of change in load with change in depth of penetration determines the stiffness of the sample.

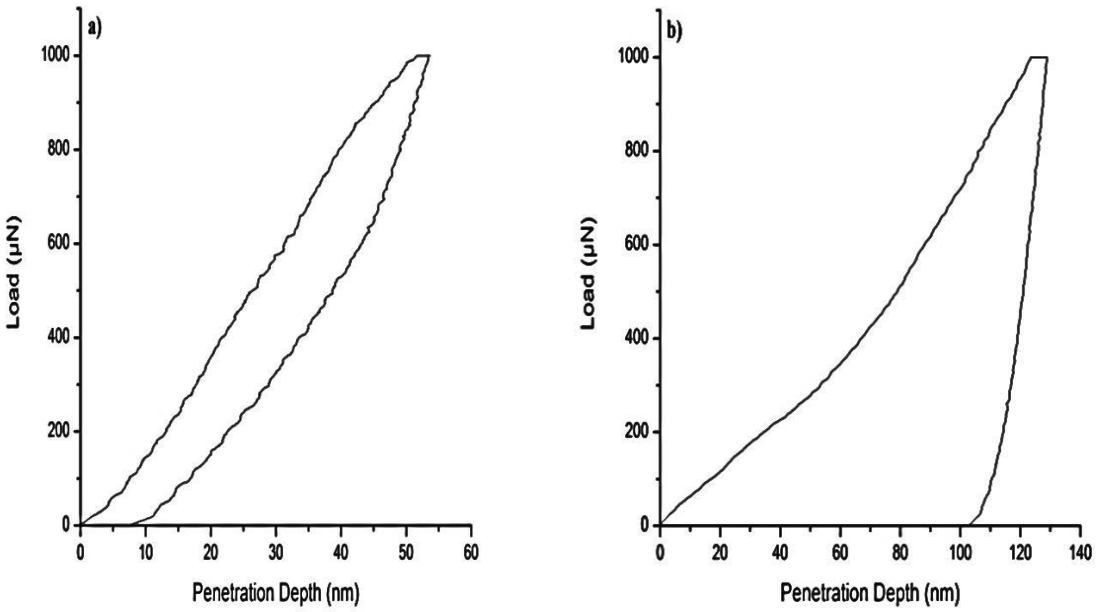

Figure 4.11: Load vs Penetration depth graph on (a) SiC particle, and (b) the matrix

The figure 4.11 describes differences between the load displacement curves of indentation on the Al- 10% wt. SiC composite at two distinct locations. One set of studies are made exactly on the reinforced particles whereas the other set is carried out in the matrix which is far away from reinforced particles. Figure 4.11 (a) is the load versus penetration curve of indentation on reinforced SiC particle. As we can see from the plot it is clear that in the loading stage, depth of penetration increases with increases in load linearly. There is no point where its curvature deflects. There is a few little pop-in events which is due to pile up of hard metal at the time of deformation. The curvature of the loading graph remains same till

it reaches the maximum loading condition. In case of unloading, due to elastic deformation the curvature is such that it tries to regain its original shape same as before the loading. So a very little final penetration depth is obtained at the end of unloading. During unloading there is sudden change in the curvature of the graph near the depth of 40 nm due to pressure induced phase change by the indenter's tip. The curvature of the nanoindentation curve on reinforced ceramic silicon carbide particles holds the very good agreement with the curvature describes by the Oliver and Pharr for hard ceramic particles [44].

In case of indentation on the matrix, curvature of the graph shows similar deformation behavior as composite but the extent at which deformation exist is different in both the cases. In case of matrix due to presence of uniformly distributed reinforce silicon carbide elastic deformation is less as compared to the pure material. The reason behind this is the strengthening behaviour of silicon carbide which restricts the movement of matrix which eventually decreases the regaining or elasticity property of the matrix. This will cause the large plastic deformation which will end up until the load reaches to its maximum value. At the maximum value of load penetration depth is maximum. In unloading curve the tip of the indenter removes from the surface slowly. At this time, material shows elastic behavior of regaining its original position but due to residual stress permanent deformation occurs on the surface in the form of indenter's impression. This deformation is less than the pure aluminum deformation but more than the reinforced silicon carbide deformation, since deformation directly relates to the depth of penetration.

So we can conclude that depth of penetration is far less in reinforced silicon carbide as compared to the matrix aluminum and pure aluminum. The depth of penetration is more in pure casted aluminum sample and matrix aluminum as compared to referred composite values. The differences in the results are shown in the mentioned Table 4.3. Vicker hardness calculated from the nanoindentation test is generally greater than the actual Vicker hardness obtained from the Micro hardness tester. The reason behind this is that the scale and method of obtaining Vickers hardness. In nanoindentation test, area is measured on the basis of penetration depth and much localized indentation which in turn helps in predicting the actual hardness of the localized zone, while in case of micro hardness test area is measured on the basis of mean of diagonal's length of indenter which averages out the deformation of both the particles and matrix. In this process, there is chance of deviation or error in estimating the impressed area from the actual area, especially in the presence of micro or nanoparticles. So this is the main reason of difference in between nonohardness and microhardness of same sample.

Table 4.3: Nanoindentation output parameters for different samples

Parameter	Al 6061	Composite	Particle
Maximum Force, F_m (μN)	1000	1000	1000
Maximum depth, h_m (nm)	137.09	117.89	53.71
Final depth, h_f (nm)	120.17	96.19	7.84
Stiffness, S (μN/nm)	74.15	74.29	33.77
Contact height, h_c (nm)	126.54	107.69	33.19
Area of contact, A_p ($nm^{2)}$	$8.15x10^5$	$5.24x10^5$	$0.91x\ 10^5$
Instrumented Hardness, H_{IT} (GPa)	1.44	1.91	10.93
Equivalent Vicker Hardness, HV Vickers	125.1	193.7	1115
Instrumented Modulus, E_{IT} (GPa)	72.78	98.95	98.95
Modulus of Elasticity, E (GPa)	72.1	88	100

4.6 Finite element Modeling of Nanoindentation test

The complete process of the Finite Element Modeling of nanoindentation test is described in this section with brief introduction to the geometry, material properties, meshing, boundary and load conditions.

Geometry: The shape of the sample is taken as a cube of length of 20 micron meter in each direction. Cube is made from extrusion of the rectangle of 20 micron in length and 20 micron in width by 20 micron meter. The Figure 4.12 also shows the notation of global coordinate systems and directions.

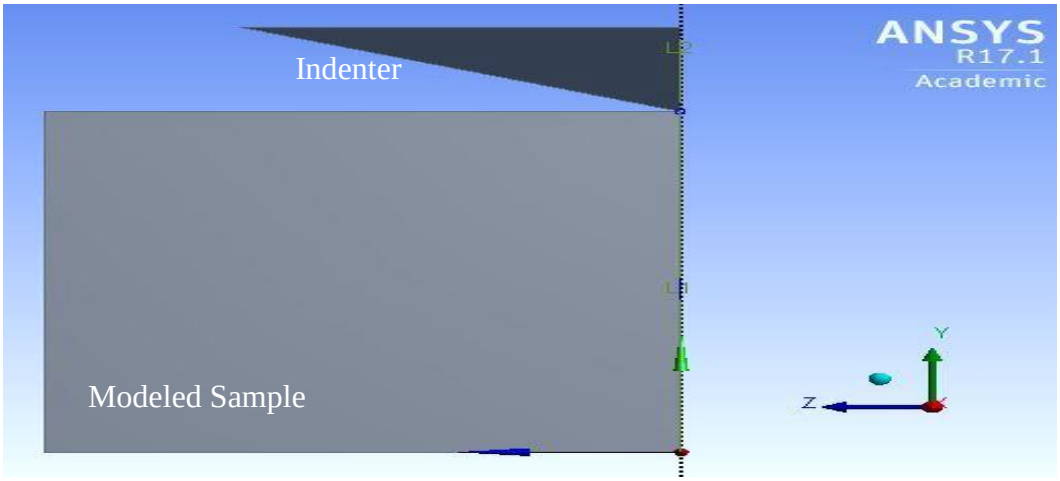

Figure 4.12: Front view of the indentation CAD model.

Indentation model is shown in Figure 4.13. The indenter had conical tip which is about 150 nm in radius. The model prepared is axisymmetric. The half space axisymmetric model is one of the first choices for many researches due to its closeness to the experimental results and least processing time [39-41].

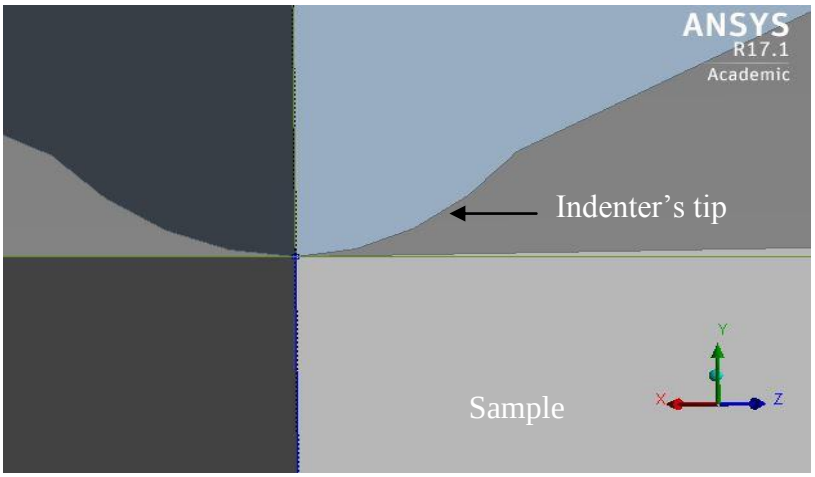

Figure 4.13: Rounded tip of modeled indenter with radius of 150 nm

The reason behind choosing the tip of the indenter rounded with 150 micron meter rather than conical sharp edge is that the previous researches reports that the sharp tip indenter holds very poor agreement with the actual results [41]. The Figure 4.14 shows the actual dimension used for modeling of indenter's tip with angle of 70.3° and radius of 150 nm.

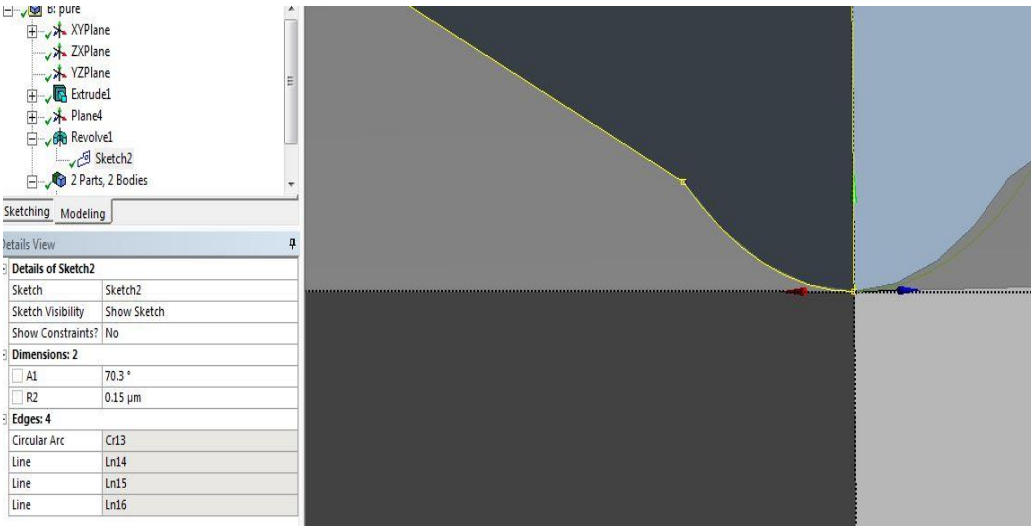

Figure 4.14: Geometry and dimensions of indenter model

Material Properties: Each and every material has its own properties and characteristics which makes it different from each other. At the time of modeling, it is very difficult to provide each and every value of properties to selected material. So it is an utmost important while modeling and simulation to input the minimum but the important material properties during material selection [41]. The minimum requirement for the material while indenting is density, elasticity and hardness. The material properties in all the models are listed in following Table 4.4.

Table 4.4: Indenter and sample's properties used for nanoindentation simulation

Materials	Young's Modulus (GPa)	Poisson's Ratio
Diamond Indenter	1140	0.07
Aluminum	72.1	0.33
Al-SiC Composite	88	0.30

The values used for diamond indenter are referred by the various researchers in their researchers [40- 41, 45]. Also the booklet provided by the Hysitron Incorporation, USA also suggested the same values and the values of composite are taken from the nano indentation result.

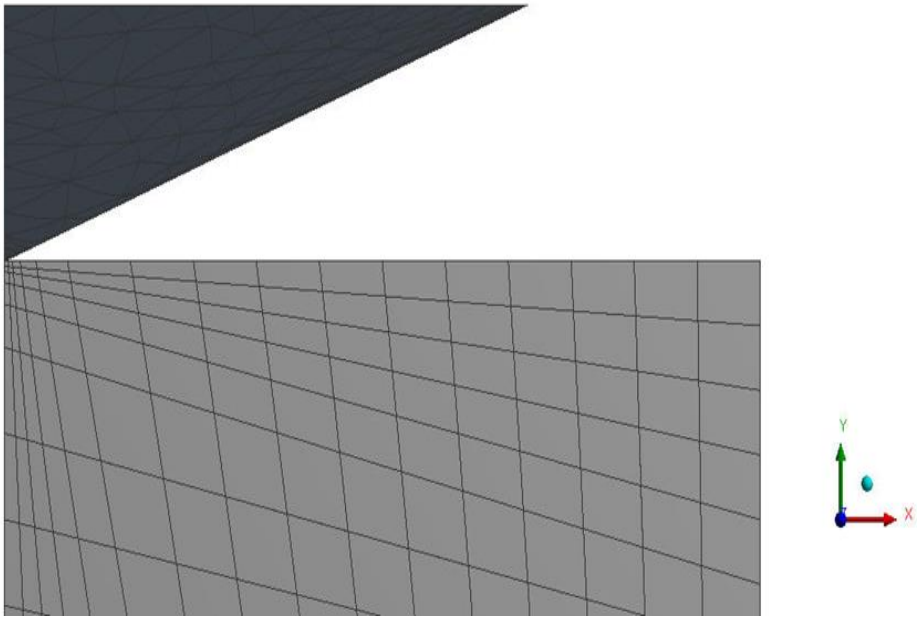

Figure 4.15: Meshing at the indenter tip and specimen

Element Meshing: Element meshing has been chosen by different fine, medium and coarse meshing based on their relevance. Meshing at the interface is fined by applying relevance at that point. Relevance across the interface increases the quality of meshing which helps the changes in contours of stress and strain distribution. At the time of meshing, element is defined through four nodes i.e. quadrilateral. Each node has two degrees of freedom for displacement in x and y direction. It also has the capability to be used for large deflection, strain, stress and plasticity. The main reason to choose this type of meshing is its compatibility with contact pairs. Mesh size is set to 10 nano-meters. The whole model contains 16942 numbers of node and 4448 are elements number. Figure 4.15 shows the meshing model of the indentation model.

Contact Pair: The connection between the indenter tip and surface of the body is made with the method provided in the analysis software. Since in actual experimentation no friction between tip and contact point, so same condition is applied in simulation. In simulations there will be no friction between indenter and surface. Targeted body is the deformable body of the sample specimen which is in contact with indenter. Contact pair is made up of two bodies one is targeted body and other is contact body as shown in the Figure 4.16.

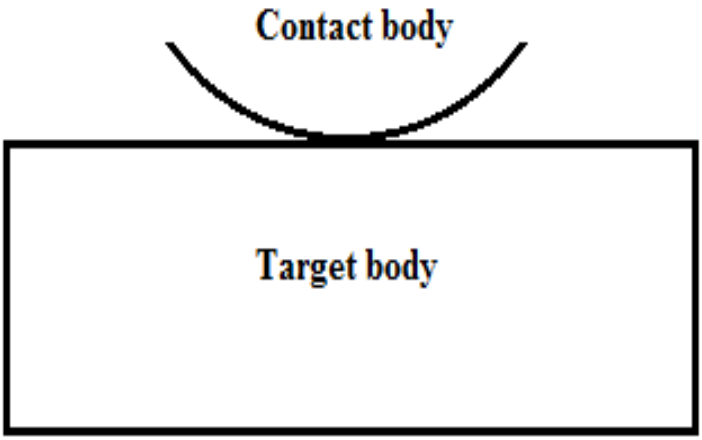

Figure 4.16: Schematic representation of Contact pair in ANSYS 17.0

Boundary Conditions: Boundary condition in any finite element method describes the restriction applied to the boundaries, nodes, faces and edges of the model. It can be applied on various types of properties like movement, pressure, velocity, force, temperature etc.

In modeling of nanoindentation process there is need to control the downward force of the indenter and position of the sample stationary. The chance of any movement of the samples from its base was removed by applying fixed boundary conditions to its bottom base. The indenter is restricted in such a manner that it moves only in up and down direction which is Y- direction in the shown Figure 4.17.

Along the vertical axis of indenter, indenter displaced only vertically i.e. in Y-direction only. X-direction displacement is set to be zero while in case of bulk material bottom side is fixed in all directions. The load applied to the indenter is the displacement load which is same as the actual experiment load. Since we applied same load variation as in actual condition so we there are 1300 points.

Loading Conditions: Load applied on the indenter in case of modeling is same as the load applied to the experimental condition. Since the experimental results also gives the loading values of force applied on the indenter that's why same values are put to the indenter. The direction of force applied on the indenter is in negative Y axis. The experimental result also gives the values till the indenter attains the condition where the tip of indenter touches the surface of sample. During this condition the loading values is in negative and not be used in simulation. So the values taken from experimental data is varies in increasing form from 0 to 1000 μN. Figure 4.17 describes the loading direction and tip of indenter where load applied.

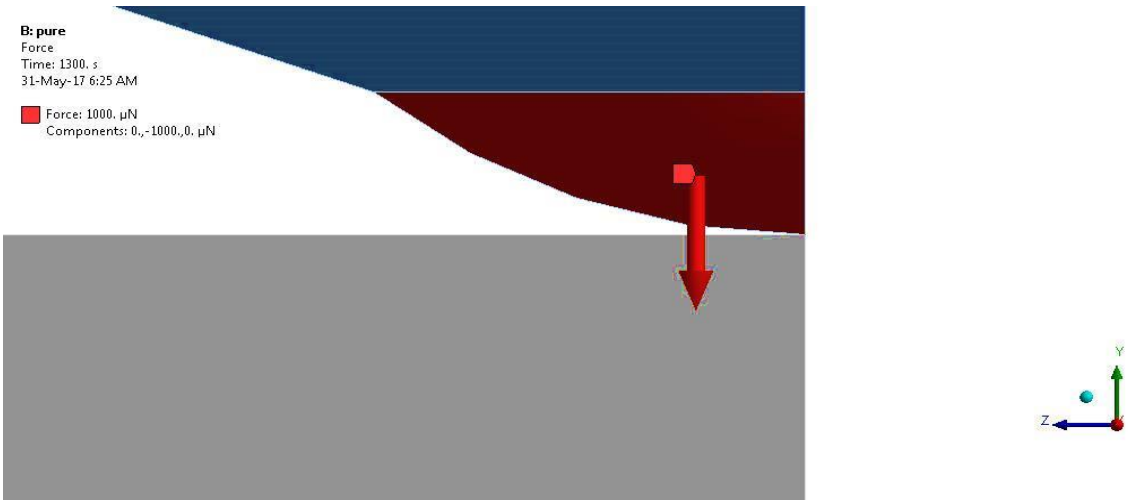

Figure 4.17: Direction of the force acting on the indenter tip

Penetration Plot: The simulation gives various results on the basis of applied boundary and loading conditions. But the results in which we are interested are the depth of penetration with time. The other results which are used cause error like measuring indent's diagonal [47]. This error depends on the material properties and increases with increases in strain increases.

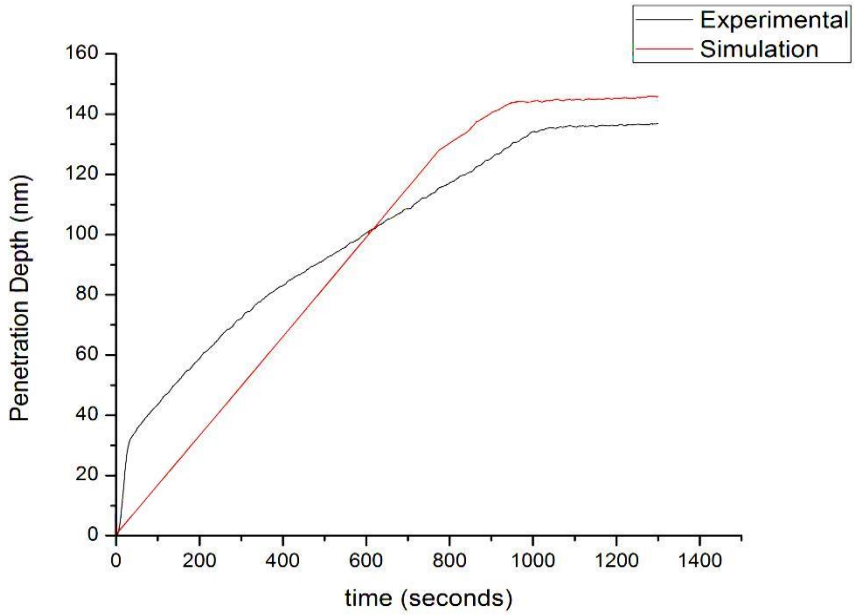

Figure 4.18: Comparison of penetration depth for pure aluminum

The hardness of the sample based on the maximum penetration depth is calculated from the formulas given by the Sneddon and Oliver-Pharr method [43-44]. In case of simulation, before determining the hardness of the metal, the contact surface area is needed to

obtain which is a function of contact depth. So contact depth is calculated with the help of maximum penetration depth. The area of contact depth is obtained from the geometrical relation given by Guillonmeau [48].While determining hardness of the sample this maximum penetration depth is used to calculate the contact area. In case of experimentation the contact area is calculated on the basis of software whereas in simulation it is calculated through the Oliver and Pharr method [44]. Comparison between experimental and simulation data are summarized in the following Table 4.5

Table 4.5: Comparison of experimental and simulation results for pure aluminum

Values	**Experimental**	**Simulation**
Maximum depth (nm)	137.09	147.63
Contact depth (nm)	126.54	143.53
Area of contact (nm^2)	$8.15x\ 10^5$	$6.56x\ 10^5$
Hardness (GPa)	1.44	1.52

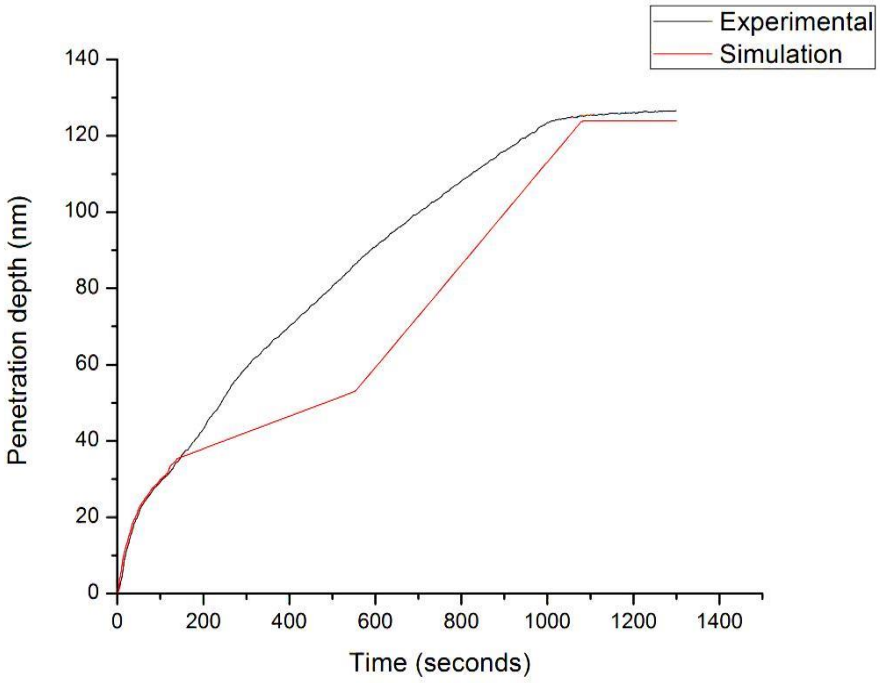

Figure 4.19: Comparison of penetration depth for composite

The graph of penetration for composite obtained from the experimental as well as simulation data is shown in Figure 4.19. As it is shown clearly in the figure, similar to the aluminum, there is a direct straight line of simulation which shows its elasticity nature and at

certain point there is a sudden change in the penetration depth till its reaches its maximum depth. Both the simulation and experimental curves hold good agreement in attaining the maximum contact depth. The maximum contact depth for experimental test is 117.89 nm while in case of 126.92 nm. The hardness of the sample based on the maximum penetration depth is calculated again from [43-44] and the area of contact depth is obtained from the geometrical relation given by Guillonmeau [48]. Summarized comparison between the experimental and simulation data are as shown in the Table 4.6.

Table 4.6: Comparison of experimental and simulation results for composite aluminum

Values	**Experimental**	**Simulation**
Maximum depth (nm)	117.89	126.92
Contact depth (nm)	107.69	116.82
Area of contact (nm^2)	5.24×10^5	4.92×10^5
Hardness (GPa)	1.91	2.03

As from the table 4.5 and 4.6, we can see that there is a good agreement of simulated data with the experimental values, indicating the suitability of implementing it for predicting the above mentioned hardness property of composite.

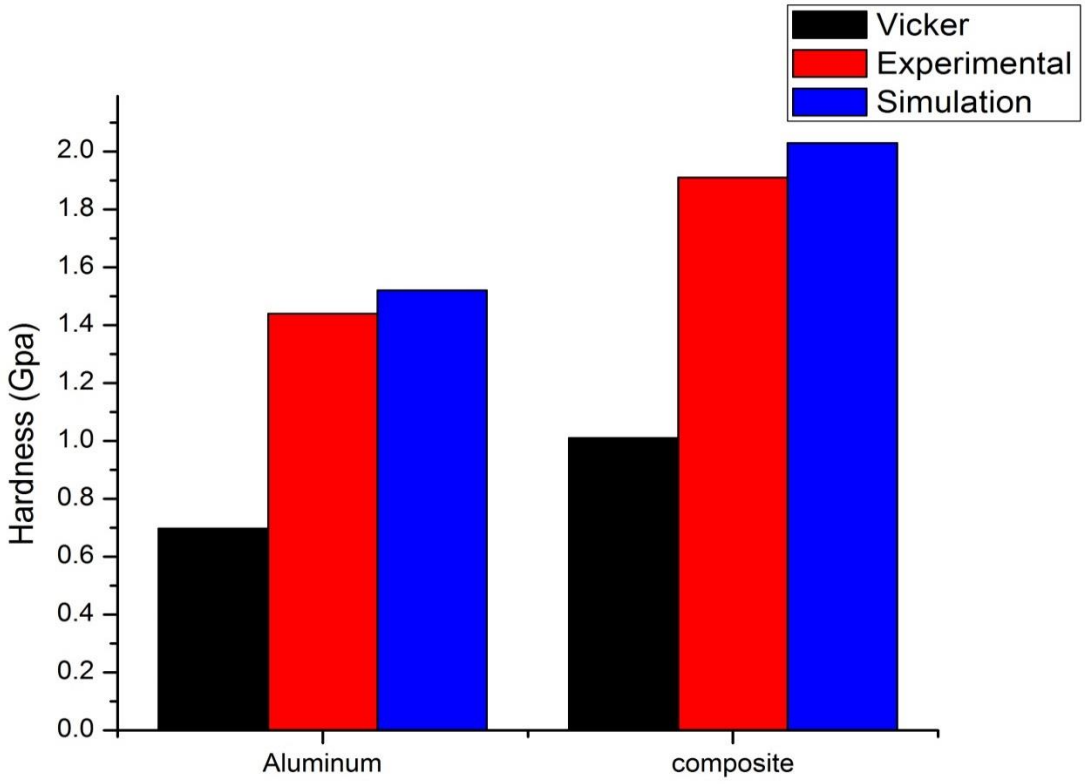

Figure 4.20: Comparing hardness obtained from differentindentation methods

Table 4.7: Micro, Nano and Simulated hardness obtained of Al and Al-SiC

Hardness (GPa)	Vicker (Converted to GPa)	Nanoindentation	Simulation
Aluminum (casted)	0.6979	1.44	1.52
Al- SiC Composite	1.011	1.91	2.01

The samples were subjected to microhardness and nanohardness testing result summarized in Table 4.7 and shown with the help of bar graph in Figure 4.7. There is 30.93% increment found in the percentage of the Vicker hardness of AMMC as compared to the cast aluminum. Minimum penetration depth is obtained in case of the reinforced silicon carbide particle due to the obvious reason of its inherent property. An increase of hardness by 24.60% as compared to the base alloy has been found from the nanoindentation results. Comparison of simulation results and experimental data show standard deviation of 1.32 for composite and0.42 for pure aluminum sample.

4.7 Image Modeling for Predicting the Mechanical Behavior against the Tensile Loading

Very few researchers tried to do work in the field of simulation of effect of shape and size of particle reinforcement in MMCs. Numerical analyses has been done by the researchers until now considered unit cell concept of regular array of reinforced particles in the matrix. However, the limitation of unit cell method includes fixed shape and size of particles (cylindrical, spherical, rectangular or cubical), spatial distribution and porosity. Accurate behavior of PRMMC can be better analyzed through simulating real microstructure in numerical model. The basic difficulties to predict macroscopic mechanical behavior lies into micro scale non homogeneity of reinforcing particle orientation and distribution. Conventional model (unit cell and experimental testing) able to provide general information of damage but intrinsic properties based on local damage characteristics are not obtained through it. Finite element methods are accurate and able to simulate different loading configurations through efficient manner in very less time. 2D models are able to capture the anisotropy of particle orientation.

Image conversion to CAD model: Composites having matrix and reinforcements with two different natures are very tedious task to model in CAD. Many researchers used mathematical probability, coding and statistical approaches to generate model for metal composite as

mentioned in literature. Image conversion is recent and trending technique to see the effect of reinforcements inside the matrix. For this in the present research work WINTOPO software is used to convert the SEM image of composite.

The detailed description about working of WINTOPO software already discussed in methodological section. Image which is in JPEG format is converted from raster to vector format. This conversion is done on the basis of canny edge detection method with the help of freeware WINTOPO software. Through this technique image which is in raster format converted into data points. This data points have lines and points with their specific positions. The conversion from raster to vector does not change or affect the image or data points. In other words the conversion is not modifying the original microstructure of the composites. With the help of this software this vector data is saved into IGESCAD file format. This IGES file is opened in the modeling software where the matrix and reinforcement are made valid for CAD model.

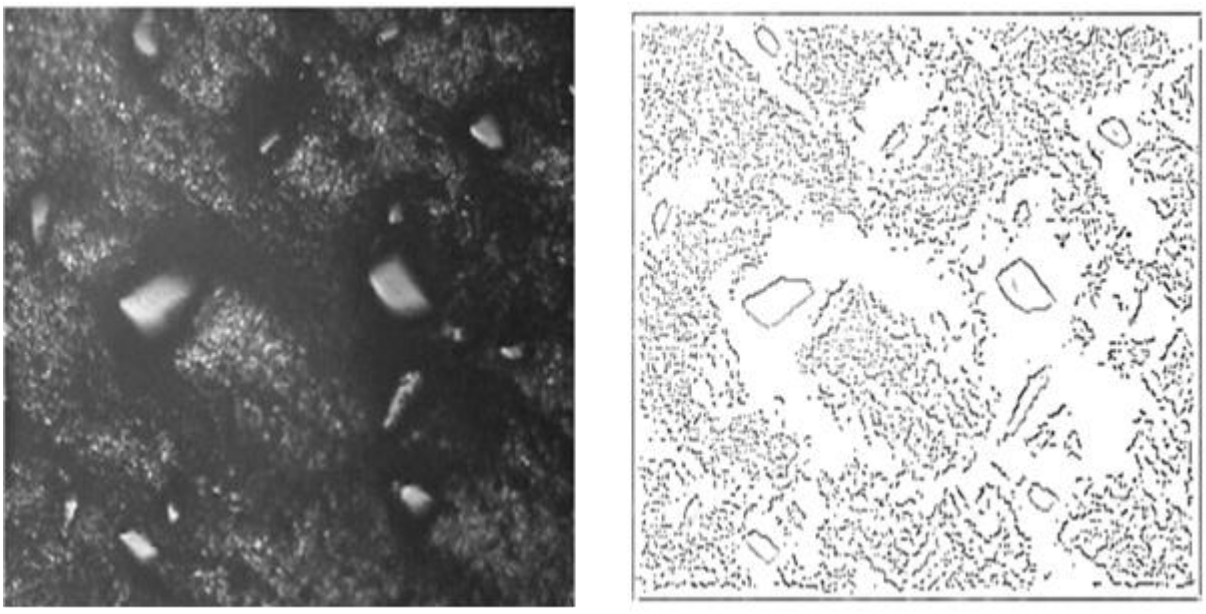

Figure 4.21: Conversion of SEM images to vector images using WINTOPO

The Figure 4.21 shows the Al-10% SiC composite conversion to vector form through software. The converted vector image shows the reinforcements and matrix clearly. Thematrix shown in the converted image seems like a mesh which surrounds the reinforcement. Reinforcements are clearly identified with the clean close boundaries. Interface of the matrix and reinforcement are seems blackish in original image due to which in converted image the surroundings of the reinforcements seems blank.

The valid model is the model which are fully closed and having no intersection in their regions. Since canny edge detection technique only makes points and lines visible inside the microstructure, there are some points where edges of the reinforcement are open. With the help of lines these edges or boundaries are made closed by combining them to closest point. After closing every entity in the CAD model, the surface is generated. First surface is generated for aluminum matrix i.e. the places except reinforcements. After that surface generation for the particles, the surface is generated through fill by selecting its closing boundaries. Each and every particle is filled with surface with same procedure. At the end, the CAD model is imported to analysis software ANSYS 17.0. Imported cad model is generated in the geometry section inside the ANSYS 17.0 as shown in Figure 4.22.

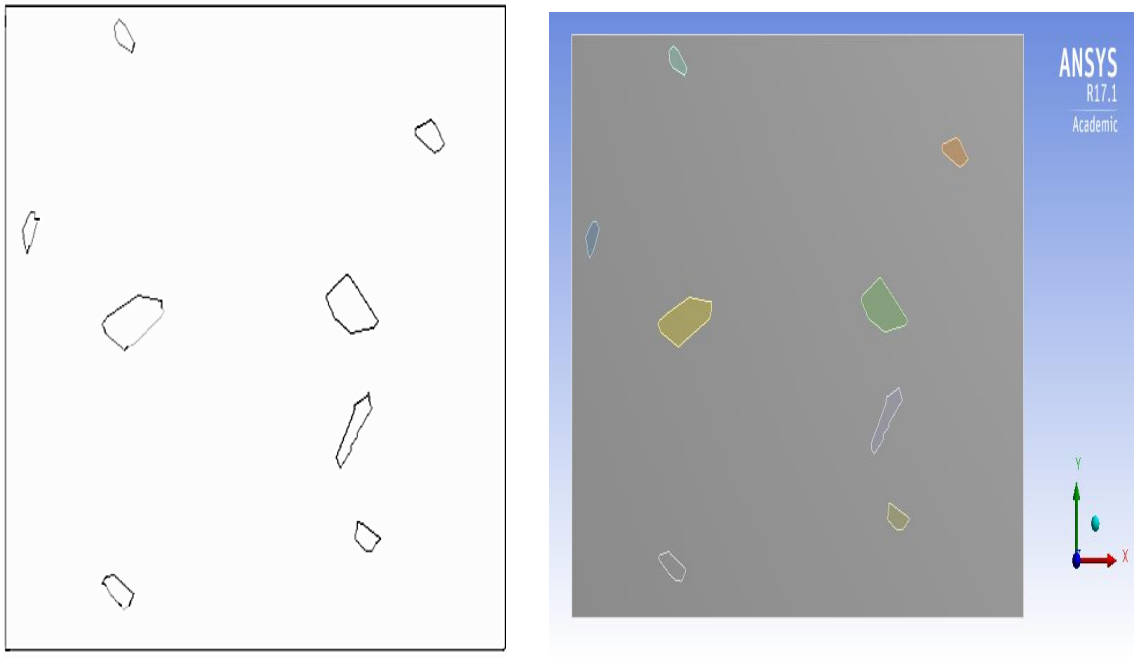

Figure 4.22: Refined closed CAD model after surface generation

Material Properties: The material properties are opted by doing intensive research on microstructure analysis of composite. All of the researches selected the same material properties which are Young's modulus and Poisson's ratio [17-27]. The selected material properties for the microstructure based image modeling are shown in Table 4.8.In our case material properties such as Young's Modulus of Aluminum matrix is taken from the nanoindentation results, while that of SiC particles are taken from the literature.

Table 4.8: Material Propertiesused for the image based modeling

Material	Young's Modulus (GPa)	Poisson's Ratio
Aluminum	72.1	0.33
Silicon Carbide	400	0.17

Mesh Generation: In this analysis element type of meshing is 4 node quadratic shapes. Two level of refinement across the reinforced elements are done to see the sudden changes in the deformation across the particle. The meshed model is shown in the Figure 4.23. Mesh at particle and matrix are attached together in such a way that it did not distorts either of the meshed components. The resulting final mesh consists of 1351 nodes and 1249 elements in model.

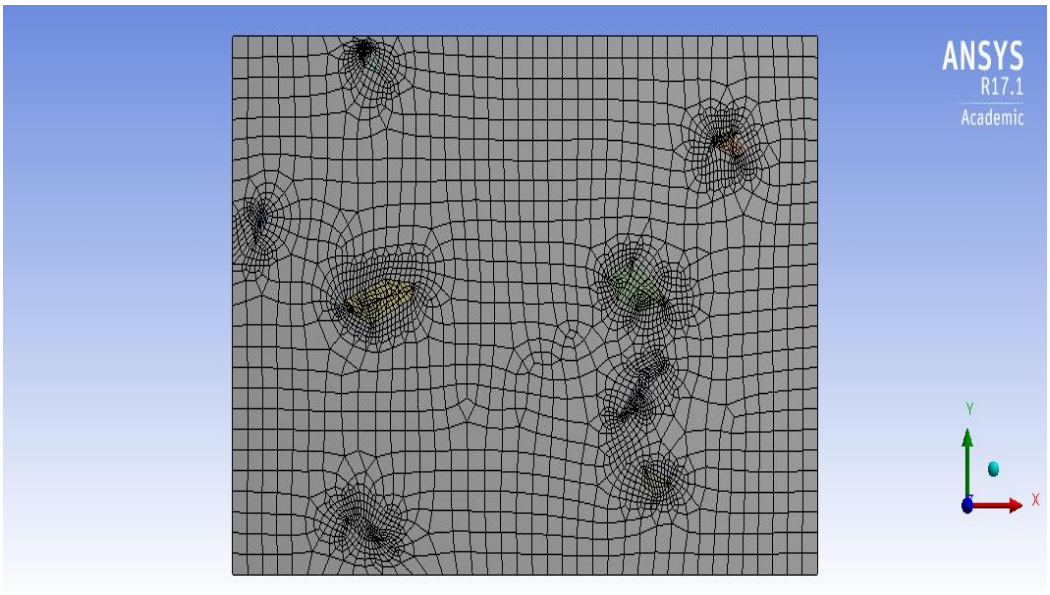

Figure 4.23: Meshing and refinement on the microstructure model

Boundary Condition: The Figure 4.24describes the boundary condition implied on the microstructure CAD model. The displacement of one end of microstructure is restricted by applying fixed end condition to the one vertical side of microstructure. The other sides are free to move in each and every direction. The applied boundary condition to microstructure model can be summarized as follows:

$$\text{At } X=0,\ U_x=0 \tag{4.1}$$

$$\text{At } X=a,\ \sigma_x=\sigma_0 \tag{4.2}$$

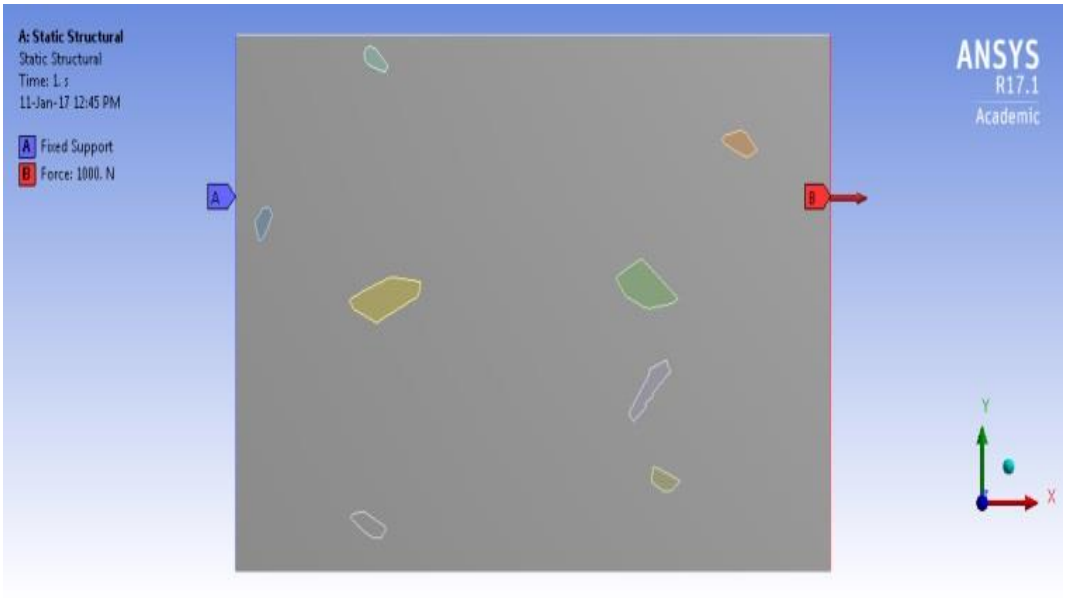

Figure 4.24: Boundary and loading condition conditions applied to the microstructure based CAD model

Loading condition: The Figure 4.24 shows the loading condition of the microstructure model. The force is applied in X direction of 1000N. The other ends are same as described in boundary conditions. The motion at the left end restricted in all directions and became fixed while at the right end uniaxial tension applied.

Simulation output results: The contour plot of stress and strain distribution of the microstructure model is shown in Figure 4.25. It is shown in the figure that the nature of equivalent von misses stress is inhomogeneous in starting due to different elastic modulus of reinforcements and matrix. The distribution of Von Misses stress shows the degree of acceptance for plastic distortion. In the clustered zones the values of von misses strain are lower than the random reinforcement region. Moreover, in some parts of the clustered regions this value is lower than the yield stress of the matrix. This in turn indicates that the plastic flow on the matrix inside the cluster is constrained resulting in considerable influence on local plasticity. Large value of stress develops near to the tip of the particles along loading axis. At high stress yielding of clustered region initiates, it means that when particles are closely allied causes constraint in plastic flow. This constraint in the flow of plasticity causes obstacles in deformation. It would initiates debonding and voids formation at the interface which eventually causes crack propagation.

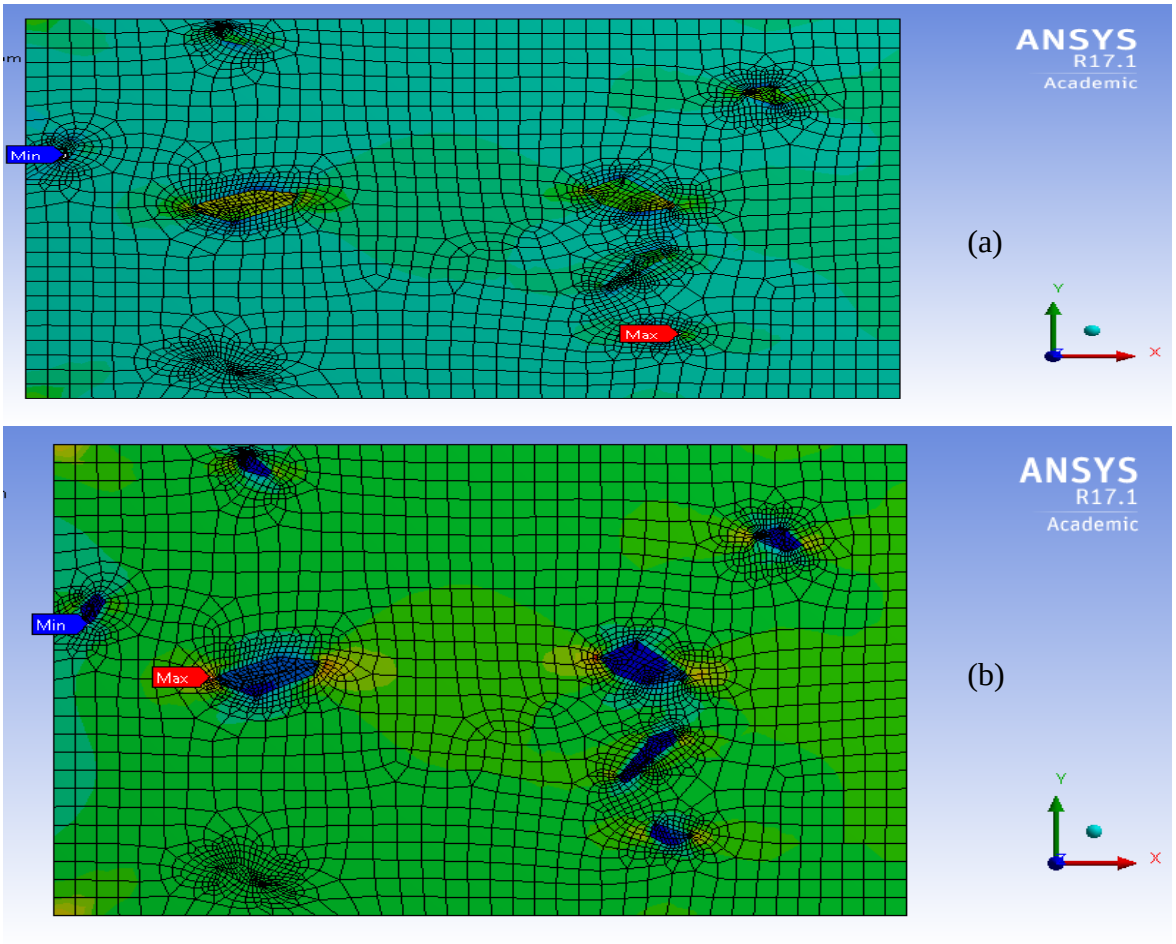

Figure 4.25: Contours of Von misses (a) stress distribution (b) strain distribution

The maximum stress occurs at the tip of reinforcement which is 266.2 MPa. However it is noted that von Misses stress at the ends of particles of SiC reaches up to their limit and cause of stress concentration. This stress concentration inside the microstructure is proportional to the particle sizes. It implies that adjacent particles yielded to higher stress and strains. From the contours it is noted that most of the load bears by the SiC particles which eventually resulted that Von Misses stresses in the particle is more than the matrix's.

The strengthening mechanism in composite is due to the load transfer of matrix to interface. Study of this interface nature is easily predicted in microstructure finite element analysis. While tensile loading large amount of loads carried by particles. In microstructure model the particles with sharp corners act as a stress concentrator and carry more amount of stress at their ends. Similarly high strain occurs at the ends of particles. Experimentally validation of the simulation phenomenon discussed with the help of deformed sample study through SEM and optical micrographs.

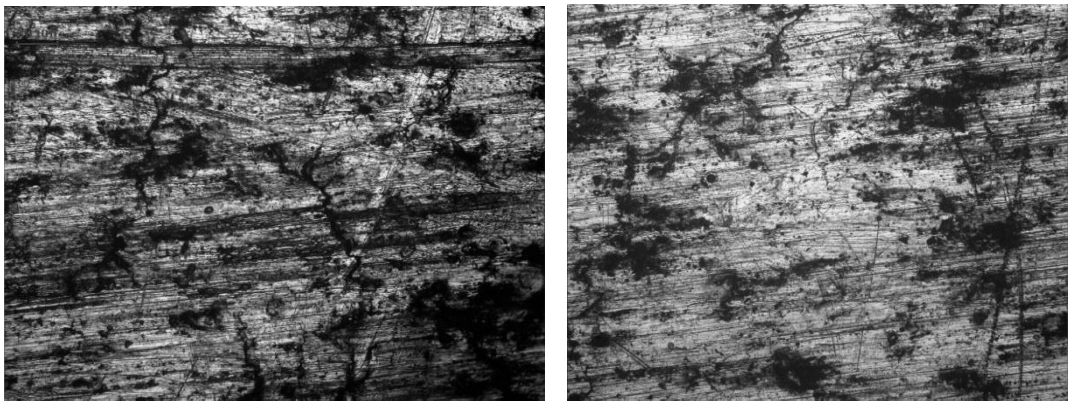

Figure 4.26: Optical micrograph of the sample subjected to tensile loading

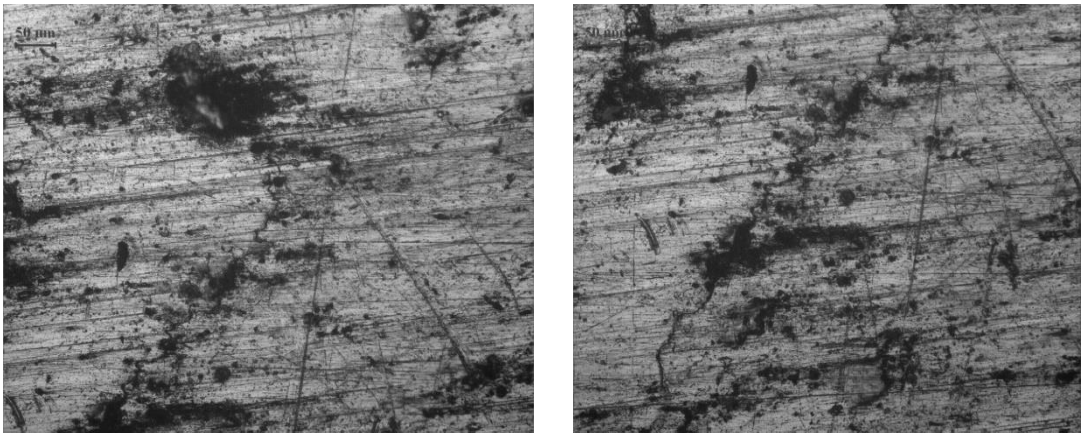

Figure 4.27: Optical micrograph of stretched sample showing crack propagation

As the both optical images (Figures 4.26 & 4.27) shows the changes in the microstructure due to elongation. Stretch marks are clearly shown in the images in a particular direction. Figure 4.26 shows the optical micrograph of the reinforced SiC particles which are disturbed or tries to elongate. The presence of the ceramic carbide into the matrix makes it brittle and causes generation of cracks surrounding the particles, which is clearly shown in the images.

Detailed analysis has been done through the SEM images obtained from the deformed surface which is shown in the Figure 4.28 and 4.29. In case of unreinforced alloys the fracture of the specimen is related with the void nucleation and growth. On microscopic examination of the fractured surface described some locally ductile and brittle mechanisms. In SEM images of the surface Figure 28 (a) shows the overall morphology of the surface. The fracture surfaces disclosed the fractured and broken particles surrounded by ductile which is known as tear ridges. These ridges are also describes as tear ridges which are related to ductile failure related in shown in the Figure 28 (b). These ridges are not in any particular

shape and very narrow. Some of the tear ridges were occurred on the surface and spread over in the form of micro voids on the surface.

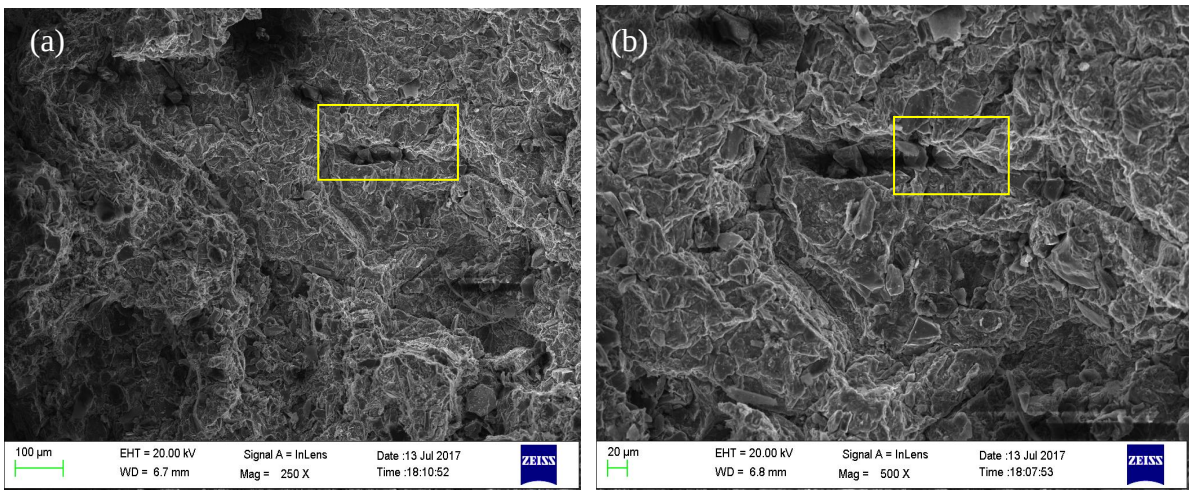

Figure 4.28: SEM micrograph showing (a) Overall morphology, (b) ductile tear ridges occurred during tensile test of Al-SiC

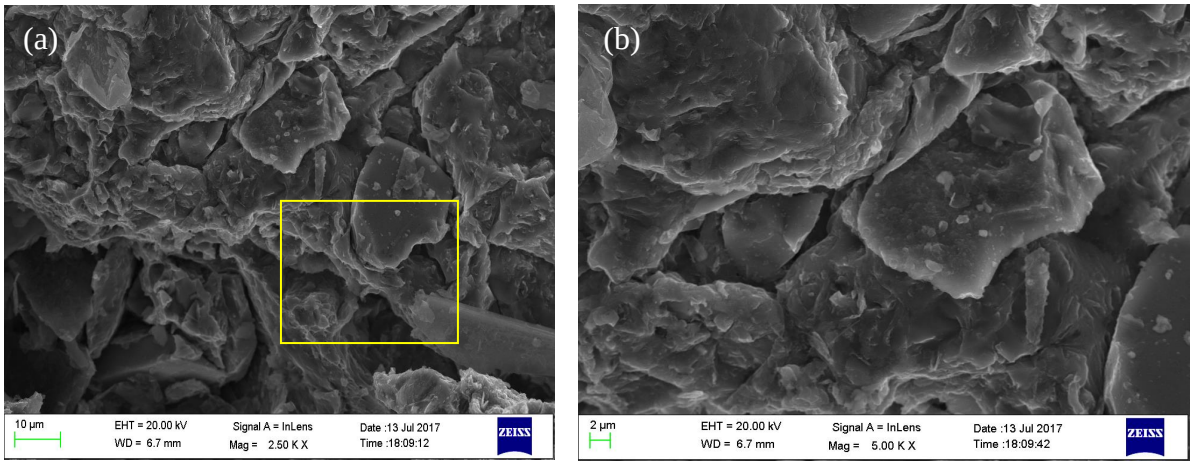

Figure 4.29: SEM images showing (a) pockets of shallow dimples on the surface, (b) cracked and decohered surface

The deformation caused by the nature of reinforced particles which are brittle and hard. They are not easily deform whereas in the soft, ductile and plastically deform aluminum metal matrix easily deformed which are shown in the Figure 29 (a) and 29 (b). The stress generates at the interface of the particle and extends to beginning of micro-voids and its growth. The main outcome of the SEM images concludes that debonding of the matrix-particle and fracture of the reinforcement. Also, great fracture was observed at the region of clustering of the particle due to generation of local stresses which was seen in the simulation

of the image modeling also. Stress occurred at the vicinity of particle are combination of local stress concentration, brittle nature of reinforcement and applied stress is responsible for cracking. The discontinuous dimples were occurred due to discontinuous nature of reinforced particle [49]. In case of clustering or agglomeration of particle the small inter-particle act as linkage to causes propagation of fracture deformation.

Comparing the experimentation SEM images results to the predicted simulations holds good agreement with each other. The propagation of cracks and voids which observed in the SEM images is near to the reinforcement particle as predicted in the simulation with the help of stress- strain distribution. The contour maps of stress strain distribution evident the occurrence of high stresses at the reinforced particle's region resulted in the form of tear and ridges as shown in the SEM images.

Chapter 5
Conclusions

5.1Work Done During the Present Research

In the present study, an attempt is made to simulate the mechanical properties and deformation behavior of composite. For this purpose the microhardness and nanohardness of the composite is taken under investigation. Along with the deformation behavior of composite under tensile loading is also investigated. The aspect of this present research is modeling of random particle reinforced metal matrix composite as same as the SEM images and detailed description of effects of particles.

Specimen's sample fabricated with liquid metallurgy of stir casting procedure. Sample's polishing and roughness are important parameters for nanoindentation test. Nanoindentation test has been successfully done on the micro size Al-SiC composite. CAD modeling and simulation have been developed for predicting the hardness of the composite. The results show the comparison of experimental and simulation results of penetration depth. Also, the effect of particle reinforcements on the deformation behavior of metal matrix composite are analysed through the stress- strain simulation through image based modeling. Experimental validation of the image based modeling simulation results is discussed with the help of SEM images of the deformed surfaces.

5.2 Major Conclusionsof the Work

From the work shown in preceding chapters and short summary mentioned in the above section the following conclusions are drawn

- SEM images validate the uniform distribution of SiC in the Al matrix of composite obtained by stir casting. Also EDS and XRD taken at the multiple location shows the abundance of reinforced material in the matrix.
- The samples were subjected to microhardness testing. There is 30.93% increment found in the percentage of the Vicker hardness of AMMC as compared to the cast aluminum.
- An increase of hardness by 24.60% as compared to the base alloy has been found from the nanoindentation results.

- However, due to the compliance produced by the plastic deformation of soft matrix mechanical properties of reinforced SiC evaluated from the nanoindentation results deviates from the actual values of the unreinforced SiC.
- Axisymmetric model is used for the simulation of nanoindentation whose results has been validated with the experimental data. Based on experiment and simulation results, hardness value has been obtained from the depth of penetration.
- Penetration plot of the experimental and simulation data are compared and holds good agreement with each other.
- Comparison of simulation results and experimental nanoindentation data show standard deviation of 1.32 for composite and 0.42for pure aluminum sample.
- Image based modeling predicts the deformation behavior of particle reinforced MMC through stress- strain distribution inside the matrix. Simulation also predicts the deformation in the form of crack generation and its propagation through the boundaries of brittle particle.
- The tear ridges and voids near the vicinity of the reinforced particle observed in the SEM images of deformed surface validate the prediction made by simulation.
- Combining both the nanoindentation simulation and microstructure image based modeling can provide a realistic approach for modeling a particle MMC.

5.3 Scope for Future Work

- This work can be further extended for the other composition as well as other metal matrix composites like aluminum boron carbide, etc. to predict hardness and other mechanical behavior.
- Similarly simulation for hardness can also be applied for various other particle reinforced MMCs.
- Methods for 3D simulation from the image based modeling can be done in future, for better understanding of behaviour of deformation.
- Further, a large scale simulation and image processing algorithm can be developed to handle a large set of reinforced particles with various morphologies and mechanical properties.

References

1. A.K. Kaw, Mechanics of Composite Materials, *CRC Taylor and Francis Group* Second addition, (2006).
2. R.F. Gibson, A review of recent research on mechanics of multifunctional composite materials and structures, *Composite Structures 92* (2010), 2793-2810.
3. G.B. Veeresh Kumar, C.S.P. Rao, N. Selvaraj, Studies on mechanical and dry sliding wear of Al6061-SiC composites, *Composites: Part B 43* (2012), 1185-1191.
4. M.K. Surappa, Aluminum matrix composites: challenges and opportunities, *Springer28* (2003), 319-334.
5. G.B. Veeresh Kumar, C.S.P. Rao, N. Selvaraj, Mechanical and tribological behavior of particulate reinforced aluminum metal matrix composites- areview, *Journal of Minerals And Materials Characterization and Engineering 10* (2011), 59-91.
6. G.J. Howell, A. Ball, Dry sliding wear of particulate reinforced aluminum alloys against automobile friction materials, *Wear 181-183* (1995), 379-390.
7. R. Tyagi, Synthesis and tribological characterization of in-situ cast Al-TiC composites, *Wear 259* (2005), 569-576.
8. J. Hashim, L. Looney, M.S.J. Hashmi, Metal matrix composites: production by the stir casting method, *Journal of Materials Processing Technology 1* (1999), 1-7.
9. P.H. Shipway, A.R. Kennedy, A.J. Wilkes, Sliding wear behavior of aluminum based metal matrix composites produced by liquid route, *Wear 216* (1998), 160-171.
10. S.K. Chaudhary, A.K. Singh, C.S. Sivaramakrishnan, S.C. Panigrahi, Wear and friction behavior of spray formed and stir cast Al-2Mg-11TiO_2, *Wear 258* (2005), 759-767.
11. R.L. Deuis, C. Subramanium, J.M. Yellup, Abrasive wear of aluminum composites- a review, *Wear 201* (1997), 132-144.
12. B. Stojanovic, L. Ivanovic, Application of aluminum hybrid composites in automotive industries, *Technical Gazette 22.1* (2015), 247-251.
13. A. Vencl, I. Bobic, Z. Miskovic, Effect of thixocasting and heat treatment on the tribological properties of hypoeutectic Al-Si alloys, *Wear 264* (2008), 61-62.
14. J. Zhang, Q. Ouyang, Q. Guo, Z. Li, G. Fan, Y. Su, L. Jiang, E.J. Lavernia, J.M. Schoenung, D. Zhang, 3D Microstructure-based finite element modeling of deformation and fracture of SiCp/Al composites, *Composite Science and Technology 123* (2016), 1-9.

15. J. Canny, A computational approach to edge detection, *IEEE transactions on pattern analysis and machine intelligence 8.6* (1986), 679-698.
16. P. Bao, L. Zhang, X. Wu, Canny edge detection enhancement by scale multiplication, *IEEE Transactions On Pattern Analysis And Machine Intelligence 27.9* (2005), 1485-1490.
17. S.B. Prabhu, L. Karunamoorthy, Microstructure-based finite element analysis of failure predication in particle-reinforced metal-matrix composite, *Journal of Materials Processing Technology 207* (2008), 53-62.
18. B.P. Kumar, S.J. Babu, Microstructure based finite element analysis for deformation behavior of aluminum metal matrix composites, *International Journal of Engineering Research and Technology 3* (2014), 2221-2223.
19. F. Ayari, E. Bayraktar, C.B. Amar, Image processing and finite element modelling for analysis of a metal matrix composite, *International Journal Of Computer Science 9* (2012), 448-458.
20. G.G. Sozhamannan, S.B. Prabhu, R. Paskaramoorthy, Failure analysis of particle reinforced metal matrix composites by microstructures based model, *Materials and Design 31* (2010), 3785-3790.
21. M. Sambathkumar, P. Navaneethakrishnan, K. Ponappa, K.S.K. Sasikumar, P. Arunkumar, Analysis of Al7075 hybrid metal matrix composite using two dimensional microstructure model based finite element method, *International Journal Of Advance Engineering Technology 7* (2016), 180-183.
22. N. Chawla and K.K. Chawla, Microstructure based modeling of the deformation behavior of particle reinforced MMC, *Journal of Material Science 41* (2006), 913-925.
23. Z. Peng, L. Fguo, Microstructure-based simulation of plastic deformation of SiC particle reinforced Al matrix composites, *Chinese Journal of Aeronautics 22* (2009), 663-669.
24. L.A. Dobrzanski, A. Silwa, T. Tanski,Finite element method application for modeling of mechanical properties, *Computational Materials Science and Surface Engineering 1* (2009), 25-28.
25. E.A. Diler, R. Ipek, An experimental and statistical effects of interaction effects of matrix particle size, reinforcement particle size and volume fraction on the flexural strength of Al-SiC_p composites by P/M using central composite design, *Materials Science and Engineering A 548* (2012), 43-55.

26. Z. Peng, L. Fu-guo, Effect of particle characteristics on deformation of particle reinforced metal matrix composites, *Transactions of Nonferrous Metals Society of China 20* (2010), 655-661.
27. A. Paknia, A. Pramanik, S. Chattopadhyaya, Effect of size, content and shape of reinforcements on metal matrix composites (MMCs) under tension, *Journal of Materials Engineering and Performance 25* (2016), 4444-4459.
28. B. Subramanian, Some considerations towards the design of wear resistant aluminum alloy, *Wear 155* (1992), 193-205.
29. N. Ramakrishnan, An analytical study on strengthening of particulate reinforced metal matrix composites, *Acta Metallurgica 44* (1996), 69-77.
30. Md. H. Rahman, H.M.M. Al-Rashed, Characterization of silicon carbide reinforced aluminum matrix composites, *Procedia Engineering90* (2014), 103-109.
31. C. Reddy, Cause and catastrophe of strengthening mechanism in 6061/Al_2O_3 composites prepared by stir casting and validation using FEA, *International Journal of Scientific Research 4.2* (2015), 1274-1281.
32. Y.X. Lu, X.M. Meng, C.S. Lee, R.K.Y. Li, C.G. Huang, J. K. L. Lai, Microstructure and mechanical behaviour of a SiC particles reinforced Al-5Cu composite under dynamic loading, *Journal of Materials Processing Technology 94* (1999), 175–178.
33. N.V. Ravi Kumar and E.S. Dwarakadasa, Effect of matrix strength on the mechanical properties of Al–Zn–Mg/SiC composite, *Composites Science and Technology 31* (2000), 1139–1145.
34. V. Jayaram, S.K. Biswas, Wear of Al2O3-SiC-(AlSi) melt oxidised ceramic composites. *Wear 225–229* (1999), 1322–1326.
35. A. Kalkanli, S. Yilmaz, Synthesis and characterization of aluminum alloy 7075 reinforced with silicon carbide particulates, *Materials and Design 29* (2008), 775–780.
36. K.K. Alaneme, A.O. Aluko, Fracture toughness (K1C) and tensile properties of as-cast and age-hardened aluminum (6063)- silicon carbide particulate composites, *Scientia Iranica 19.4* (2012), 992–996.
37. J.S.S. Babu, C.G. Kang, Nanoindentation behaviour of aluminum based hybrid composite with graphite nanofiber/alumina short fiber, *Materials and Design 31* (2010), 4881-4885.
38. J.S.S Babu, C.G. Kang, Nanomechanical properties of magnesium- based hybrid composites with graphite nanofiber and alumina short fiber, *Journal of Composite Materials 45.25* (2011), 2685-2695.

39. A. Pramanik, L.C. Zhang, J.A. Arsecularatne, Micro-indentation of metal matrix composite- an FEM investigation, *Trans Tech Publications 340-341* (2007), 563-570.
40. J. Rodriguez, M.A.G. Maneiro, P. Poza, M.T.G. Rio, Determination of mechanical properties of aluminum matrix composites constituents, *Materials Science and Engineering A437* (2006), 406-412.
41. A. Waigh, A. Fathy, Experimental investigation and FE simulation of nano-indentation on Al-Al_20_3 nanocomposites, *Advanced Powder Technology 27.2* (2016), 403-410.
42. Aluminum Standards and Data 2000 and/or International Alloy Designations and Chemical Composition Limits for Wrought Aluminum and Wrought Aluminum Alloys (Revised 2001).
43. I.N. Sneddon, The relation between load and penetration in the axisymmetric boussinesq problem for a punch of arbitrary profile, *International Journal Engineering Science* 3 (1965), 47-57.
44. W.C. Oliver, G.M. Pharr, An improved technique for determining hardness and elastic modulus using load and displacement sensing indentation measurements, *Journal of Material Research 7.6* (1992), 1564-1583.
45. K.D. Bouzakis, N. Michailidis, G. Skordaris, Hardness determination by means of a FEM- supported and applications in thin hard coatings, *Surface and Coatings Technology 200* (2005), 867-871.
46. M.F. Doerner, W.D. Nix, A method for interpreting the data from depth sensing instruments, *Journal of Material Research 1.4* (1986), 601-609.
47. M. Spychalski, T. Wejrzanowski, K.J. Kurzydłowski, Materials hardness estimation by simulation of the indentation process, *Solid State Phenomena 129* (2007), 119-124.
48. G. Guillonneau, G. Kermouche, S. Bec, J.L. Loubet, Determination of mechanical properties by nanoindentation independently of indentation depth measurement, *Journal of Materials Research 27* (2012), 2551-2560.
49. T.S. Srivatsan, M. Hajri, C. Smith, M. Petraroli, The tensile response and fracture behavior of 2009 aluminum alloy metal matrix composite, *Materials Science and Engineering A36* (2003), 91-100.

Research Outcomes

Conference:

- Shivam Saini, Hiralal Bhowmick, "Deformation Behavior of Particulate Metal Matrix Composite", Presented at National Conference on Innovative Trends in Mechanical Engineering (NCITME- 2017) in collaboration with Indian Institution of Industrial Engineering, Shri Mata Vaishno Devi University, Katra, Jammu and Kashmir, India, 4th March 2017.

Journals:

- Shivam Saini, Hiralal Bhowmick, "Nanoindentation and Microstructural Image Based FEM Simulation to Predict the Hardness and Deformation Behaviour of Particle reinforced AMMC". Manuscript Submitted in Journal of Materials Engineering and Performance.